Research article

JHEP|Reports

Effect of pegbelfermin on NASH and fibrosis-related biomarkers and correlation with histological response in the FALCON 1 trial

Elizabeth A. Brown,[1,†] **Anne Minnich**,[1,†] Arun J. Sanyal,[2] Rohit Loomba,[3] Shuyan Du,[1] John Schwarz,[1] Richard L. Ehman,[4] Morten Karsdal,[5] Diana J. Leeming,[5] Giovanni Cizza,[1] Edgar D. Charles[1,*]

[1]*Bristol Myers Squibb, Princeton, NJ, USA;* [2]*Virginia Commonwealth University, Richmond, VA, USA;* [3]*University of California, San Diego, San Diego, CA, USA;* [4]*Mayo Clinic College of Medicine, Rochester, MN, USA;* [5]*Nordic Bioscience, Biomarkers & Research, Herlev, Denmark*

JHEP Reports **2023.** https://doi.org/10.1016/j.jhepr.2022.100661

Background & Aims: FALCON 1 was a phase IIb study of pegbelfermin in patients with non-alcoholic steatohepatitis (NASH) and stage 3 fibrosis. This FALCON 1 *post hoc* analysis aimed to further assess the effect of pegbelfermin on NASH-related biomarkers, correlations between histological assessments and non-invasive biomarkers, and concordance between the week 24 histologically assessed primary endpoint response and biomarkers.
Methods: Blood-based composite fibrosis scores, blood-based biomarkers, and imaging biomarkers were evaluated for patients with available data from FALCON 1 at baseline through week 24. SomaSignal tests assessed protein signatures of NASH steatosis, inflammation, ballooning, and fibrosis in blood. Linear mixed-effect models were fit for each biomarker. Correlations and concordance were assessed between blood-based biomarkers, imaging, and histological metrics.
Results: At week 24, pegbelfermin significantly improved blood-based composite fibrosis scores (ELF, FIB-4, APRI), fibrogenesis biomarkers (PRO-C3 and PC3X), adiponectin, CK-18, hepatic fat fraction measured by MRI-proton density fat fraction, and all four SomaSignal NASH component tests. Correlation analyses between histological and non-invasive measures identified four main categories: steatosis/metabolism, tissue injury, fibrosis, and biopsy-based metrics. Concordant and discordant effects of pegbelfermin on the primary endpoint *vs*. biomarker responses were observed; the most clear and concordant effects were on measures of liver steatosis and metabolism. A significant association between hepatic fat measured histologically and by imaging was observed in pegbelfermin arms.
Conclusions: Pegbelfermin improved NASH-related biomarkers most consistently through improvement of liver steatosis, though biomarkers of tissue injury/inflammation and fibrosis were also improved. Concordance analysis shows that non-invasive assessments of NASH support and exceed the improvements detected by liver biopsy, suggesting that greater consideration should be given to the totality of available data when evaluating the efficacy of NASH therapeutics.
Clinical trial number: Post hoc analysis of NCT03486899.
Impact and implications: FALCON 1 was a study of pegbelfermin *vs*. placebo in patients with non-alcoholic steatohepatitis (NASH) without cirrhosis; in this study, patients who responded to pegbelfermin treatment were identified through examination of liver fibrosis in tissue samples collected through biopsy. In the current analysis, non-invasive blood- and imaging-based measures of fibrosis, liver fat, and liver injury were used to determine pegbelfermin treatment response to see how they compared with the biopsy-based results. We found that many of the non-invasive tests, particularly those that measured liver fat, identified patients who responded to pegbelfermin treatment, consistent with the liver biopsy findings. These results suggest that there may be additional value in using data from non-invasive tests, along with liver biopsy, to evaluate how well patients with NASH respond to treatment.
© 2023 The Author(s). Published by Elsevier B.V. on behalf of European Association for the Study of the Liver (EASL). This is an open access article under the CC BY-NC-ND license (http://creativecommons.org/licenses/by-nc-nd/4.0/).

Introduction

Non-alcoholic steatohepatitis (NASH) is the advanced, progressive form of non-alcoholic fatty liver disease (NAFLD) and is defined by the presence of ≥5% hepatic steatosis along with hepatocyte injury, with or without fibrosis.[1] Of the histological characteristics of NASH, fibrosis has been shown to be the most predictive in terms of all-cause and disease-specific mortality;[2,3] patients with bridging fibrosis (NASH Clinical Research Network [CRN] fibrosis stage 3) have an increased risk of disease-related adverse events relative to patients with stage 1 or 2 fibrosis.[4] Currently, no pharmacological treatments are approved for NASH, and the associated clinical and economic burdens are expected to continue to rise in the coming years.[5]

The pathophysiology of NASH is complex and multifactorial, with a metabolic component and additional drivers that can lead to hepatocyte stress, inflammation, cell death, and fibrosis.[6,7] Because of the complexity and heterogeneity of NASH, a range

Keywords: fibroblast growth factor 21; non-alcoholic steatohepatitis; liver fibrosis; steatosis; precirrhotic NASH; SomaSignal.
Received 22 April 2022; received in revised form 3 November 2022; accepted 7 December 2022; available online 7 January 2023
† These authors contributed equally to this work.
* Corresponding author. Address: 3401 Princeton Pike, Princeton, NJ, USA, 08648.
E-mail address: Edgar.Charles@bms.com (E.D. Charles).

of clinical tests may be necessary to dynamically monitor disease. In clinical trials, the gold-standard method for monitoring NASH progression is through histological analysis of liver biopsy tissue; however, this is not feasible in routine clinical practice for numerous reasons, including the patient risk associated with performing repeated biopsies and potential erroneous estimation of disease-related changes due to biopsy timing, sampling variability due to the heterogeneity of fibrosis throughout the liver, and scoring variability.[8–10] As a result, an unmet need remains for robust, non-invasive means of characterizing dynamic changes in disease activity and assessing treatment response in patients with NASH and advanced fibrosis.

At present, numerous non-invasive measures of fibrosis and NASH disease activity are routinely used in the clinic and incorporated into clinical trials. These assessments include blood-based composite fibrosis scores, namely enhanced liver fibrosis (ELF), fibrosis-4 (FIB-4), and aspartate aminotransferase (AST)-to-platelet ratio index (APRI), which, though not designed for monitoring treatment response, have recently been used to evaluate treatment efficacy and less commonly, to monitor disease, in patients with NASH.[11–13] Additionally, serum concentrations of monomeric and crosslinked forms of a disintegrin and metalloproteinase with thrombospondin motifs 2 [ADAMTS-2]-released N-terminal type III collagen propeptide (PRO-C3 and PC3X, respectively) are biomarkers of fibrogenesis; increased PRO-C3 concentrations have been associated with increasing fibrosis stage, lobular inflammation, and ballooning as well as progressive liver fibrosis.[14–17] Furthermore, the imaging techniques MRI-proton density fat fraction (MRI-PDFF) and magnetic resonance elastography (MRE) measure hepatic fat fraction and stiffness, respectively, and a ≥30% relative reduction in hepatic fat fraction measured by MRI-PDFF has been associated with histological NASH improvement in secondary analyses of the phase II MOZART and FLINT studies.[18,19] Because of the association between MRI-PDFF and histological response, early-phase NASH trials have employed MRI-PDFF as an endpoint to evaluate therapeutic efficacy.[13] A set of novel NASH component composite panels that are measurable in blood and enable simultaneous analysis of several features of NASH pathophysiology have also been investigated for disease-monitoring capability.[20] Further investigation of these non-invasive tests and others are needed to understand which tests will be useful for the assessment of treatment responses and to monitor disease progression over the longer term.

Fibroblast growth factor 21 (FGF21) is a non-mitogenic hormone that regulates aspects of metabolism including glucose and lipid homeostasis,[21,22] and modulates secretion of adiponectin, an adipokine with insulin-sensitizing, antisteatotic, anti-inflammatory, and antifibrotic properties.[23,24] Pegbelfermin (PGBF), a recombinant, polyethylene glycol-conjugated analogue of human FGF21, has an extended half-life compared with endogenous FGF21 and supports up to weekly dosing in clinical trials.[25,26] In the phase IIb FALCON 1 study, 24-week PGBF treatment in patients with NASH and stage 3 fibrosis was associated with higher rates of fibrosis improvement without NASH worsening or NASH improvement without fibrosis worsening (24%-31% across the 10 mg, 20 mg, and 40 mg dose arms) compared with placebo (14%), though the trial did not meet the primary endpoint because of a lack of dose-dependent response rate differentiation.[27] In addition, patients treated with PGBF had improvements in non-invasive measures of steatosis, injury/inflammation, and fibrosis.

This exploratory *post hoc* analysis of FALCON 1 was designed to further test the holistic effects of PGBF on biomarkers of NASH disease activity and fibrosis at week 24, which allowed for the direct comparison of biopsy-based and non-invasively measured treatment responses.

Patients and methods

FALCON 1 primary study design

FALCON 1 (NCT03486899) was a randomized, phase IIb, multicenter, double-blind, placebo-controlled study conducted in the United States and Japan; detailed FALCON 1 trial design and primary study results have previously been published.[27,28] Briefly, eligible patients were 18 to 75 years of age with a liver biopsy specimen that was consistent with NASH and stage 3 liver fibrosis per NASH CRN criteria and had a score of ≥1 for each NAFLD activity score (NAS) component (steatosis, lobular inflammation, and ballooning). The number of patients with a NAS of <4 was limited such that it comprised no more than 15% of the total randomized population. Patients were ineligible if they had any liver disease other than NASH, or current or past hepatocellular carcinoma, liver transplant, or hepatic decompensation. Randomized patients (1:1:1:1) received placebo or PGBF (10 mg, 20 mg, or 40 mg) once weekly via subcutaneous injections during the 48-week double-blind treatment period. The primary endpoint, measured at week 24, was a ≥1 stage fibrosis improvement (*i.e.*, ≥1 stage decrease in NASH CRN fibrosis score) without worsening of NASH (*i.e.*, increase in NAS by ≥1 point) or NASH improvement (*i.e.*, decrease in NAS by ≥2 points with contribution from at least 2 NAS components) without worsening of fibrosis (*i.e.*, increase in NASH CRN fibrosis score by ≥1 stage) as determined by liver biopsy.

Assessments

Liver biopsy specimens were collected at week 24 (±7 days) for comparison with biopsy specimens collected up to 6 months prior to or during screening. Histological scoring was performed by the blinded central pathologist using NASH CRN fibrosis and NAS criteria. Imaging evaluations of hepatic fat fraction (by MRI-PDFF) and liver stiffness (by MRE) were performed at baseline and at week 24; all study images were analyzed by a central imaging facility.

Blood samples were collected every 4 weeks (±5 days) from day 1 to week 24 after at least 8 h of fasting (except for alanine aminotransferase [ALT], AST, and platelets) for measurement of serum- and plasma-based biomarkers. Non-invasive composite scores of fibrosis (FIB-4, APRI, and ELF) were calculated using the following parameters: FIB-4: patient age, AST and ALT concentrations, and platelet counts; APRI: AST concentrations and platelet counts; ELF: hyaluronic acid, procollagen-3 N-terminal propeptide (P3NP), and tissue inhibitor of metalloproteinases type 1 (TIMP-1) concentrations measured via immunoassay (Labcorp Drug Development, Burlington, NC, USA). PRO-C3 and PC3X concentrations were evaluated using ELISAs developed by Nordic Bioscience (Herlev, Denmark).[17,29] Adiponectin concentration was measured by Myriad RBM (Austin, TX, USA) using Luminex immunoassays. HDL, LDL, and triglyceride measurements were obtained from blood samples obtained after ≥8 h of fasting. Caspase-cleaved cytokeratin 18 (CK-18 M30) concentration was assessed by Nexelis (Laval, Canada) using ELISA.

SomaSignal tests (SomaLogic, Boulder, CO, USA) for NASH ballooning, lobular inflammation, steatosis, and fibrosis[20] were

performed at baseline, week 12, and week 24. For each NASH component, composite scores were compiled from individual scores for a panel of 5 to 14 blood-based protein biomarkers. Data were expressed as probability scores and the changes in probability scores from baseline to weeks 12 and 24 were calculated. Patients with probability scores ≥50% for each metric were predicted to have more severe fibrosis or higher NAS component scores.[20,30] Detailed SomaSignal test scoring definitions and protein analyte composition are shown in Table S1.

Statistical analyses

For pharmacodynamic modeling, linear mixed-effect models were fit for each biomarker using the lmer function from the lmerTest 3.1-3 package in R.[31] Measurements were regressed on time and treatment arm, including an interaction between time and treatment and a random effect for each patient: measurement ∼ time + treatment + time:treatment + 1|patient. Mean change from baseline and 95% CIs were provided for each biomarker throughout the study. Adjusted *p* values comparing placebo with the individual or combined PGBF dose arms were calculated for the week 24 timepoint using glht in the multcomp 1.4-15 package in R; *p* values were corrected for multiple testing using the Benjamini-Hochberg procedure across all tests and biomarkers. Pairwise canonical correlations were calculated using cancor in the stats 4.0.3 package in R; correlation coefficients were then clustered hierarchically by Euclidean distance. *P* values were calculated by permutation testing using p.perm in the CCP 1.1 package in R; those correlations with $p \leq 0.1$ after Benjamini-Hochberg correction were reported as absolute values. Correlations, including some that were non-significant, were represented by color on the heatmap.

For the concordance analysis, primary endpoint responses and non-responses were coded as binary −1 and 1, respectively. Change from baseline for all biomarkers and data types was scaled to have variance of 1, keeping 0 centered at no change from baseline. For inclusion in this analysis, patients were required to have complete biopsy data at baseline and week 24 (N = 179) and also ≥50% of all data types at both baseline and at week 24. The data for these remaining 173 patients were clustered hierarchically using Euclidean distance on the x-axis; data for biomarkers, imaging, biopsy, and the primary endpoint were also clustered hierarchically using Euclidean distance on the y-axis. The clustering and heatmap were created using Heatmap from the ComplexHeatmap 2.6.2 package in R.

Percentage change from baseline in hepatic fat fraction measured by MRI-PDFF was calculated for all patients. To evaluate hepatic fat fraction measured by MRI-PDFF as a non-invasive biomarker to monitor changes in absolute fat percentage measured histologically, a linear mixed-effect model was fit using the lmer function from the lmerTest 3.1-3 package in R. The change from baseline in absolute fat percentage was regressed on baseline hepatic fat fraction by MRI-PDFF, the change from baseline in hepatic fat fraction by MRI-PDFF, and treatment arm (including an interaction between change from baseline in hepatic fat fraction and treatment) and adjusted for the covariates of age, sex, and type 2 diabetes (T2D) status: change from baseline in absolute fat percentage ∼ MRI-PDFF baseline + MRI-PDFF change from baseline + treatment + MRI-PDFF change from baseline:treatment + age + sex + T2D. *P* values and coefficients for the estimated effect of changes in hepatic fat fraction by MRI-PDFF on change in absolute fat percentage for individual PGBF dose arms and placebo were calculated using glht in the multcomp 1.4-15 package in R. Pearson correlations were also calculated using the stats package in R.

Correlations between the continuous change in biomarkers at week 24 and the ordinal change in NASH CRN fibrosis stage or total NAS at week 24 were assessed using Kendall's tau. *P* values were adjusted for multiple testing using the Benjamini-Hochberg procedure.

Results

Baseline FALCON 1 patient characteristics

In the primary FALCON 1 study, 197 patients were randomized 1:1:1:1 to the four study arms. Patient characteristics and baseline demographics were similar across study arms.[27] Most patients were White (85.3%) and female (58.9%) and the total study population had a mean age of 56.9 years, mean body mass index of 35.6 kg/m^2, and mean hemoglobin A1c level of 6.9%. For all arms combined, the mean hepatic fat fraction measured by MRI-PDFF was 13.2%, the mean baseline liver stiffness measured by MRE was 4.4 kPa, and the mean PRO-C3 concentration was 19.4 μg/L (Table 1).

Effect of PGBF on NASH-related biomarkers

Adiponectin concentrations, which are generally low in patients with NASH compared to healthy patients, have been shown to be inversely correlated with severity of steatosis.[23] In the PGBF arms, mean adiponectin concentrations peaked at week 4 and the highest concentration was observed in the 40 mg PGBF arm (Fig. 1A). Mean concentrations declined at subsequent time points but remained significantly increased from baseline to week 24 in the 10 mg and 40 mg PGBF arms compared with placebo. Additional metabolic readouts measured in the study were plasma lipids; increased concentrations of HDL have been associated with NASH resolution.[32] At week 24, PGBF arms had numerically greater increases in mean HDL and numerically greater decreases in mean LDL concentrations compared with placebo (Fig. S1).

Relative levels of hepatocyte apoptosis, which is observed as a result of NASH-related liver injury and disease progression, can be estimated by measuring serum levels of the caspase-cleaved fragment of CK-18 (M30, the caspase-cleaved fragment of the main intermediate filament protein found in hepatocytes).[33,34] In the placebo arm, mean CK-18 M30 concentrations were lowest at week 4 and then increased through week 24 (Fig. 1B). In all PGBF arms, mean CK-18 M30 concentrations decreased from baseline beginning at week 4 and were significantly reduced from baseline to week 24 compared with placebo.

ELF, FIB-4, and APRI are composite scores that identify patients who are most likely to have advanced fibrosis.[35,36] Compared with placebo, 20 mg and 40 mg PGBF treatment significantly reduced mean FIB-4 and APRI scores from baseline to week 24 (Fig. 1C). Mean baseline ELF scores were similar among arms and were in the upper range for patients with stage 3 fibrosis. The mean ELF score at week 24 was significantly decreased from baseline in PGBF arms in a dose-dependent manner relative to placebo; concentrations of hyaluronic acid, P3NP, and TIMP-1 were all reduced from baseline relative to placebo, though the differences were significant only for P3NP and TIMP-1 at week 24 (Fig. S2).

The circulating extracellular matrix biomarkers PRO-C3 and PC3X are generated during the formation and accumulation of

Table 1. Mean baseline biomarker values.

Parameter, mean (95% CI)	Placebo n = 49	10 mg PGBF n = 49	20 mg PGBF n = 50	40 mg PGBF n = 49
Composite fibrosis scores				
n	48	49	50	48
ELF	10.21 (9.94–10.48)	10.00 (9.72–10.28)	10.04 (9.79–10.29)	10.15 (9.85–10.44)
Hyaluronic acid, μg/L	136.40 (83.93–188.88)	113.07 (80.85–145.29)	111.01 (83.47–138.55)	136.26 (94.26–178.25)
P3NP, μg/L	12.84 (11.39–14.28)	12.02 (10.65–13.39)	12.36 (10.93–13.79)	12.33 (10.95–13.71)
TIMP-1, μg/L	295.94 (269.39–322.49)	290.87 (265.99–315.76)	278.37 (260.23–296.52)	303.32 (274.45–332.18)
n	47	48	48	47
FIB-4	2.01 (1.67–2.36)	1.80 (1.55–2.04)	1.72 (1.44–1.99)	2.06 (1.73–2.39)
n	47	48	48	47
APRI	0.79 (0.59–0.99)	0.69 (0.59–0.79)	0.66 (0.52–0.80)	0.75 (0.63–0.88)
Fibrogenesis biomarkers				
n	49	49	50	49
PRO-C3, μg/L	18.99 (16.40–21.57)	18.93 (16.56–21.31)	20.11 (16.80–23.43)	19.45 (16.99–21.91)
n	49	49	50	49
PC3X, μg/L	14.64 (12.25–17.03)	14.52 (12.08–16.96)	13.63 (11.58–15.68)	13.01 (11.14–14.89)
Tissue injury biomarker[a]				
n	48	48	48	46
CK-18 M30, U/L	500.94 (364.97–636.90)	577.98 (416.07–739.89)	482.83 (354.60–611.06)	464.80 (392.62–536.98)
Imaging assessments				
n	41	44	47	45
Hepatic fat fraction (MRI-PDFF), %	12.46 (10.66–14.26)	13.86 (11.99–15.73)	13.38 (11.59–15.17)	12.99 (11.47–14.50)
n	40	39	44	42
Liver stiffness (MRE), kPa	4.28 (3.89–4.66)	4.56 (3.99–5.12)	4.08 (3.76–4.40)	4.57 (4.09–5.04)
SomaSignal tests[b]				
n	49	49	50	49
NASH steatosis, %	75 (66–83)	76 (68–83)	80 (74–87)	72 (64–81)
n	49	49	50	49
NASH inflammation, %	59 (49–63)	54 (46–61)	54 (47–61)	52 (45–60)
n	49	49	50	49
NASH ballooning, %	67 (61–73)	69 (64–74)	66 (60–72)	67 (61–74)
n	49	49	50	49
NASH fibrosis, %	74 (69–79)	72 (66–78)	72 (68–77)	76 (70–82)
Metabolic biomarkers				
n	49	49	50	49
Adiponectin, mg/L	4.06 (3.49–4.63)	4.37 (3.63–5.10)	3.61 (3.07–4.15)	4.24 (3.35–5.12)
n	49	49	50	49
HDL, mg/dl	44.0 (41.0–47.2)	47.9 (44.5–51.4)	44.3 (41.0–47.6)	45.0 (41.4–49.1)
n	49	49	50	49
LDL, mg/dl	100.4 (91.3–109.8)	104.1 (94.7–113.7)	108.9 (97.4–120.7)	107.1 (95.9–118.3)

ADAMTS-2, a disintegrin and metalloproteinase with thrombospondin motifs 2; ALT, alanine aminotransferase; APRI, AST-to-platelet ratio index; AST, aspartate aminotransferase; CK-18 M30, caspase-cleaved cytokeratin 18; ELF, enhanced liver fibrosis; FIB-4, fibrosis-4; MRE, magnetic resonance elastography; MRI-PDFF, MRI-proton density fat fraction; NASH, non-alcoholic steatohepatitis; P3NP, procollagen-3 N-terminal propeptide; PC3X, crosslinked ADAMTS-2-released N-terminal type III collagen propeptide; PGBF, pegbelfermin; PRO-C3, monomeric ADAMTS-2-released N-terminal type III collagen propeptide; TIMP-1, tissue inhibitor of metalloproteinases type 1.

[a] Baseline AST and ALT values are reported with the primary study results.[27]

[b] Probability scores ≥50% are considered predictive of greater severity.

collagen during fibrogenesis.[15,17] In the placebo arm, mean concentrations of both biomarkers increased from baseline to week 24 (Fig. 1D) and reductions in mean concentrations of PRO-C3 and PC3X were observed in all PGBF arms beginning at week 4. At week 24, the mean changes in PRO-C3 and PC3X concentrations from baseline were significantly lower in all PGBF arms compared with the placebo arm.

The quantitative imaging techniques MRI-PDFF and MRE are used to measure hepatic fat fraction and liver stiffness, respectively, in patients with NAFLD/NASH.[13] At week 24, mean liver stiffness in the 10 mg and 40 mg PGBF arms was numerically lower compared with baseline; conversely, mean liver stiffness in the placebo and 20 mg PGBF arms was numerically greater than at baseline (Fig. 2). Compared with the placebo arm, the pooled PGBF arms had a reduction in mean hepatic fat fraction from baseline; this reduction was most pronounced in the 10 mg PGBF arm.

Effect of PGBF treatment on SomaSignal NASH components

SomaSignal tests detect patterns of protein signatures in blood that are predictive of histological disease severity in NASH steatosis, inflammation, ballooning, and fibrosis.[20,30] At week 24, mean SomaSignal scores for all four NASH components were significantly reduced in all PGBF-treated arms compared with placebo (Fig. 3). Mean reductions in ballooning, inflammation, and fibrosis at week 24 were dose dependent across the PGBF-treated arms. In patients who received 10 mg, 20 mg, and 40 mg of PGBF, respectively, this translated to a 6%, 8%, and 14% lower relative probability of having more severe inflammation (*i.e.*, score of ≥2 for NAS lobular inflammation); an 11%, 16%, and 18% lower probability of having more severe ballooning (*i.e.*, score of ≥1 for NAS ballooning); and a 6%, 8%, and 9% lower probability of having significant fibrosis (*i.e.*, NASH CRN stage ≥2), respectively, compared with those who received placebo.

Clustering among non-invasive biomarkers and biopsy-based analyses

Canonical correlation and clustering by Euclidean distance were performed to assess the extent to which empirical data confirmed putative mechanistic categories of NASH-related biomarkers. At

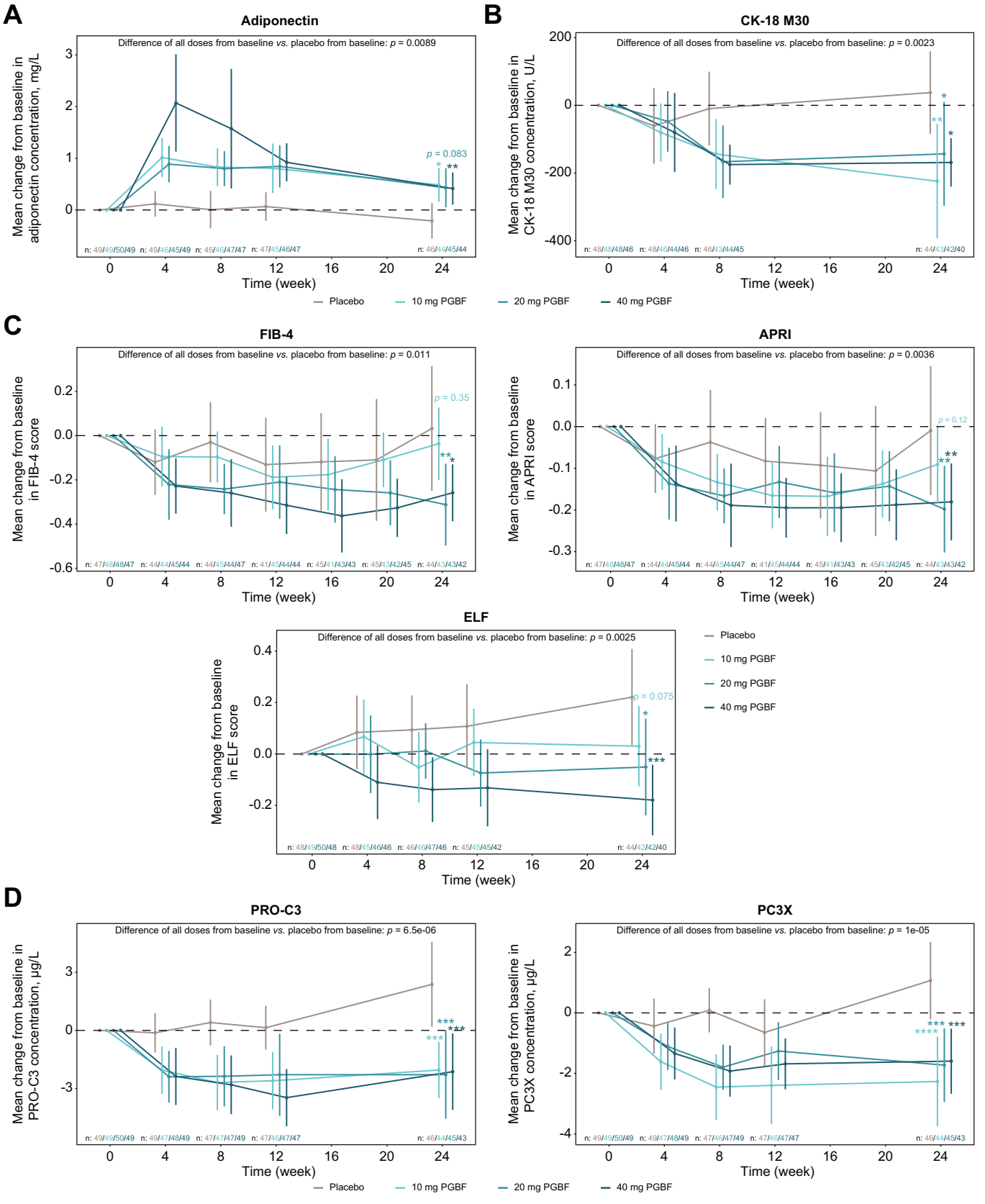

Fig. 1. Mean absolute change from baseline in steatosis, tissue injury, and fibrosis biomarkers. Mean changes from baseline ± 95% CI are shown. *P* values were corrected for multiple testing across all tests and biomarkers using the Benjamini-Hochberg procedure. *$p \leq 0.05$; **$p \leq 0.01$; ***$p \leq 0.001$; ****$p \leq 0.0001$. ADAMTS-2, a disintegrin and metalloproteinase with thrombospondin motifs 2; APRI, aspartate aminotransferase-to-platelet ratio index; CK-18 M30, caspase-cleaved cytokeratin 18; ELF, enhanced liver fibrosis; FIB-4, fibrosis-4; MRE, magnetic resonance elastography; MRI-PDFF, MRI-proton density fat fraction; PC3X, crosslinked ADAMTS-2-released N-terminal type III collagen propeptide; PGBF, pegbelfermin; PRO-C3, monomeric ADAMTS-2-released N-terminal type III collagen propeptide.

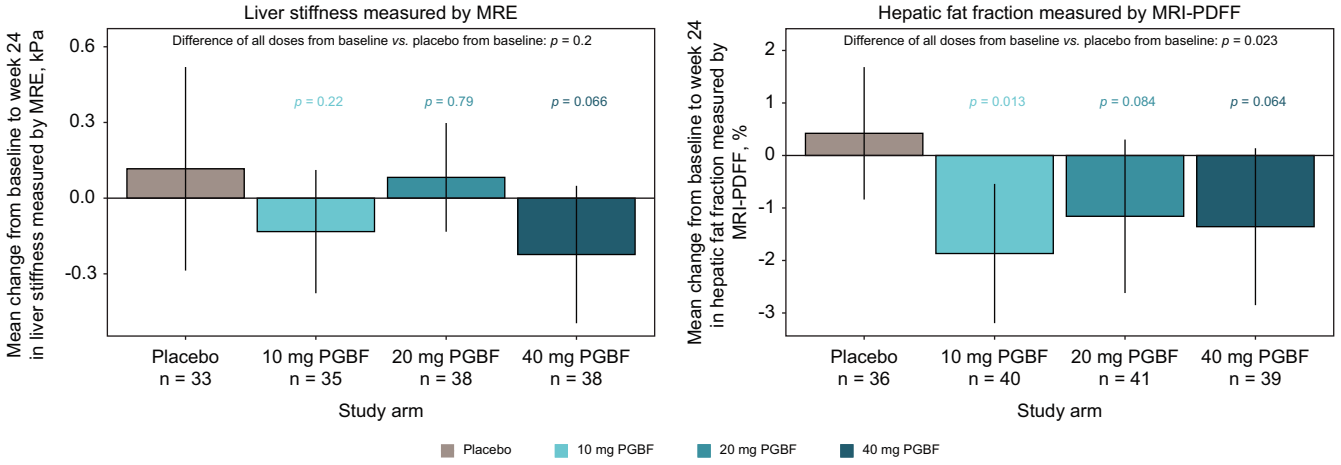

Fig. 2. Non-invasive imaging assessments of hepatic steatosis and stiffness. Mean changes from baseline ± 95% CI are shown. *P* values were corrected for multiple testing across all tests and biomarkers using the Benjamini-Hochberg procedure. MRE, magnetic resonance elastography; MRI-PDFF, MRI-proton density fat fraction; PGBF, pegbelfermin.

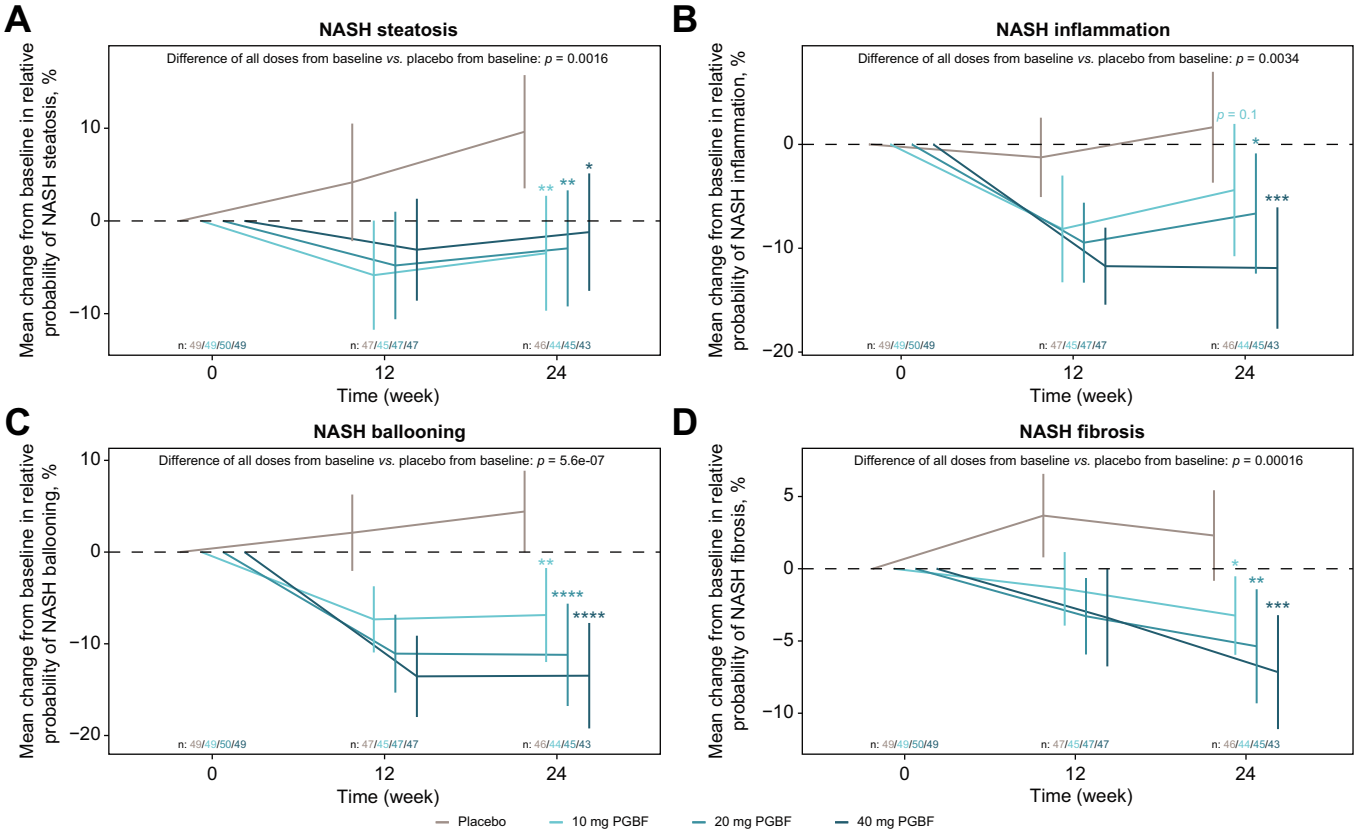

Fig. 3. Mean absolute change from baseline in NASH SomaSignal tests. Mean ± 95% CI are presented; probability scores are expressed as percentages. Probability scores of ≥50% are considered predictive of more severe steatosis, inflammation, ballooning, or fibrosis. Adjusted *p* values were corrected for multiple testing by the Benjamini-Hochberg procedure. **p* ≤0.05; ***p* ≤0.01; ****p* ≤0.001; *****p* ≤0.0001. NASH, non-alcoholic steatohepatitis; PGBF, pegbelfermin.

week 24, four main correlation clusters were observed. The most distinct cluster was of steatosis-related measures (Fig. 4) and included absolute fat percentage, hepatic fat fraction measured by MRI-PDFF, SomaSignal steatosis, and other blood-based metabolic biomarkers (adiponectin, HDL, and triglycerides). A second cluster consisting of fibrosis-related measures was observed and included liver stiffness measured by MRE, ELF, FIB-4, and the blood-based biomarkers PRO-C3 and PC3X. A third cluster of liver injury/inflammation measures included AST, ALT, and CK-18 M30. The fourth cluster primarily included biopsy-based metrics.

The primary endpoint was correlated with its defining biopsy-based metrics (ρ = 0.3 with NAS steatosis; ρ = 0.4 with

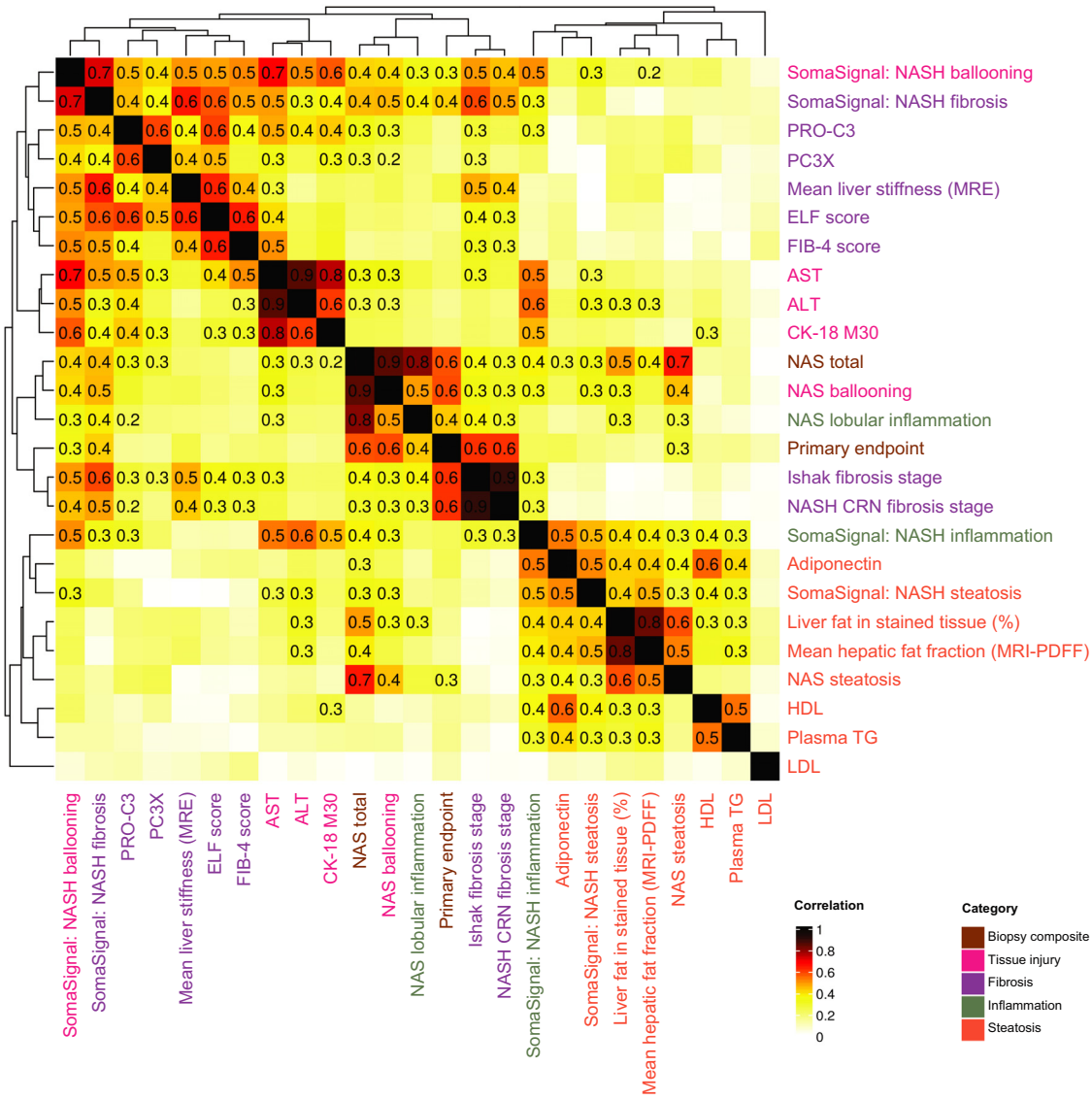

Fig. 4. Clustering of correlation coefficients for week 24 biomarkers and histological assessments. Canonical correlation across all non-invasive and histological metrics for 179 patients were plotted by heatmap color. Correlations with adjusted *p* values ≤0.1 after Benjamini-Hochberg correction were printed; clustering by Euclidean distance was performed on correlation coefficients. ALT, alanine aminotransferase; AST, aspartate aminotransferase; CK-18 M30, caspase-cleaved cytokeratin 18; ELF, enhanced liver fibrosis; FIB-4, fibrosis-4; MRI-PDFF, MRI-proton density fat fraction; NAS, non-alcoholic fatty liver disease activity score; NASH, non-alcoholic steatohepatitis; PC3X, crosslinked ADAMTS-2-released N-terminal type III collagen propeptide; PRO-C3, monomeric ADAMTS-2-released N-terminal type III collagen propeptide; TG, triglycerides.

NAS inflammation; ρ = 0.6 with NAS ballooning, NAS total, NASH CRN fibrosis score, and Ishak fibrosis stage) and was also moderately correlated with SomaSignal ballooning and fibrosis (ρ = 0.3 and 0.4, respectively). The biopsy-based metrics showed modest correlation with blood-based biomarkers corresponding to their functional category (*e.g.*, Ishak score correlated with ELF score; NAS ballooning correlated with AST). NASH CRN and Ishak fibrosis scores were also moderately correlated with mean MRE value (ρ = 0.4–0.5) and SomaSignal ballooning and fibrosis scores (ρ = 0.4–0.6).

The liver injury cluster showed modest correlation with the blood-based fibrosis biomarkers (*e.g.*, AST correlated with PRO-C3 [ρ = 0.4–0.5] and PC3X [ρ = 0.3]). SomaSignal ballooning scores were moderately to strongly correlated with the tissue injury biomarkers AST, ALT, and CK-18 M30 (ρ = 0.7, 0.5, and 0.6, respectively) and moderately correlated with all of the blood-based biomarkers of fibrosis (*e.g.*, AST correlated with PRO-C3 [ρ = 0.5] and ELF [ρ = 0.4]). SomaSignal fibrosis scores showed slightly stronger correlation with fibrosis biomarkers (ρ = 0.6 with MRE and ELF; ρ = 0.4 with PRO-C3 and PC3X) and slightly weaker correlation with tissue injury/inflammation biomarkers (ρ = 0.5 with AST; ρ = 0.4 with CK-18 M30; and ρ = 0.3 with ALT). SomaSignal inflammation scores were moderately correlated with tissue injury/inflammation biomarkers (ρ = 0.6 with ALT; ρ = 0.5 with AST and CK-18 M30) and modestly to moderately correlated with steatosis biomarkers (ρ = 0.5 with adiponectin and SomaSignal steatosis; ρ = 0.3–0.4 with absolute fat percentage, hepatic fat fraction by MRI-PDFF, HDL, and triglycerides)

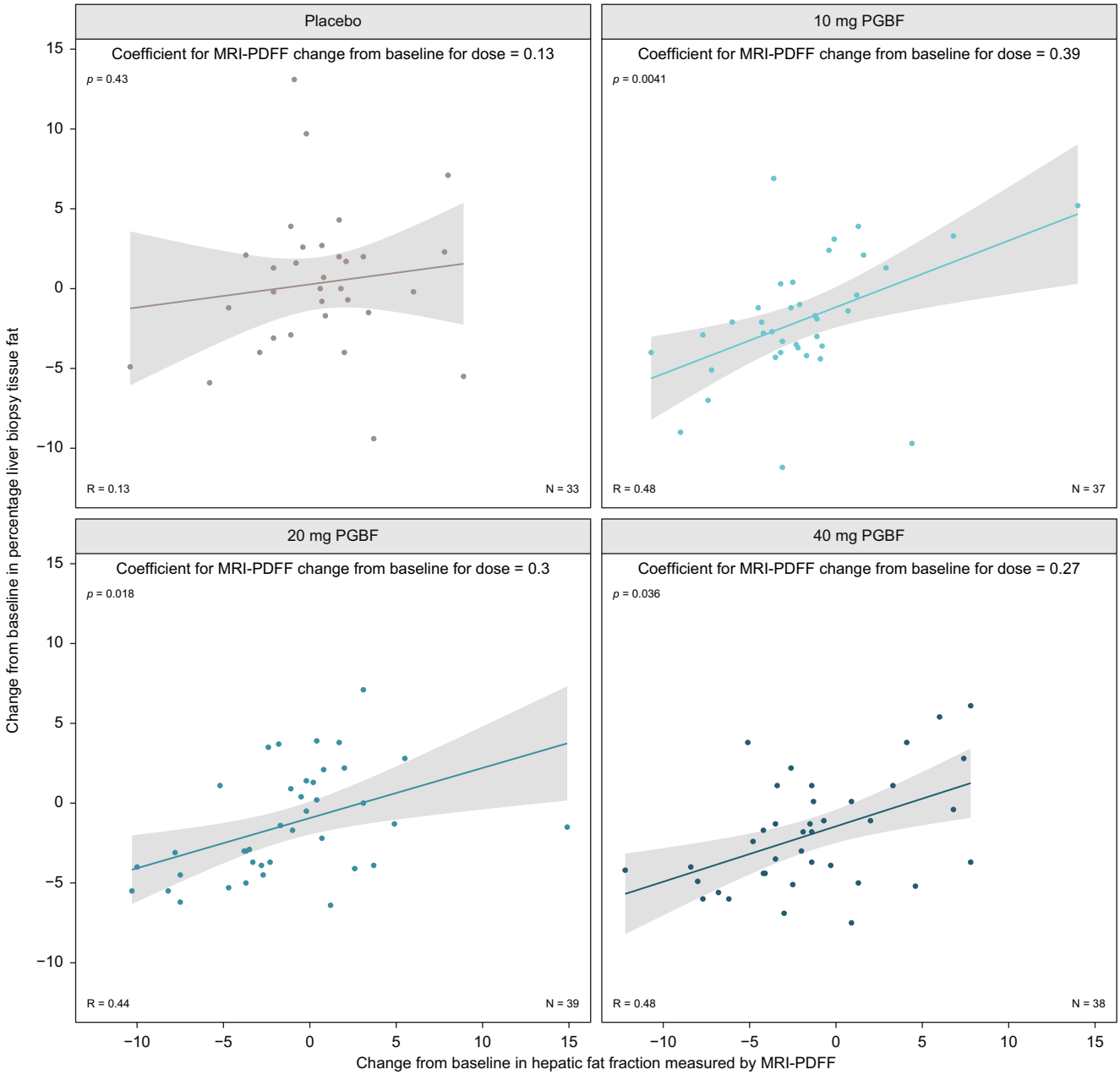

Fig. 5. Week 24 change in hepatic fat fraction by MRI-PDFF *vs.* change in absolute hepatic fat percentage. A linear mixed model was fit for histologically-assessed hepatic fat fraction (liver biopsy tissue fat) change from baseline on hepatic fat fraction measured by MRI-PDFF change from baseline, treatment, and an interaction between the two. Coefficients represent the estimated effect of a given change in hepatic fat fraction by MRI-PDFF on the predicted change in histologically-assessed hepatic fat fraction for a given treatment arm. *p* values provide the significance of the coefficient for each treatment arm. MRI-PDFF, magnetic resonance imaging-proton density fat fraction; PGBF, pegbelfermin.

but were not significantly correlated with the histologically assessed lobular inflammation NAS component.

The strong correlation at week 24 between measurements of hepatic fat by MRI-PDFF and by histological evaluation was further evaluated given the antisteatotic effect of PGBF. From baseline to week 24, changes in hepatic fat fraction measured by MRI-PDFF were significantly associated with absolute fat percentage in patients who received PGBF (10 mg: p = 0.0041; 20 mg: p = 0.018; 40 mg: p = 0.036) but not placebo (p = 0.43; Fig. 5), where changes in steatosis did not rise above experimental noise. Furthermore, MRI-PDFF measured larger reductions in hepatic fat fraction compared with the histological measurement with a 1% reduction in MRI-PDFF corresponding to an approximate reduction of 0.27% to 0.39% in absolute fat percentage, depending on the treatment arm.

Concordance of primary endpoint response with biomarker responses

Beyond the association of antisteatotic changes in patients who received PGBF, the concordance of treatment response for several categories of histological, imaging, and blood-based biomarkers was also assessed for each patient; four main

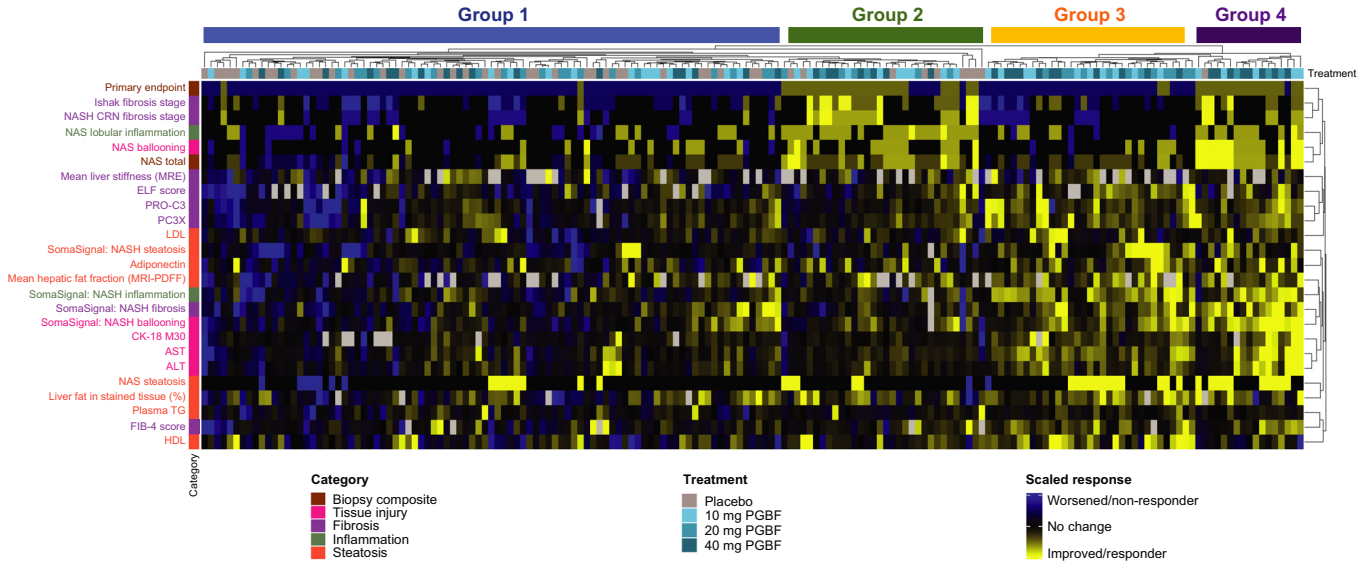

Fig. 6. Concordance analysis between primary endpoint and biomarker responses. Clustering on the primary endpoint (responders [yellow] were scored −1; non-responders [blue] were scored +1) and scaled biomarker data (variance normalized to 1) was performed by Euclidean distance. Visual patient groups are denoted above the heat map. ALT, alanine aminotransferase; AST, aspartate aminotransferase; CK-18 M30, caspase-cleaved cytokeratin 18; CRN, Clinical Research Network; ELF, enhanced liver fibrosis; FIB-4, fibrosis-4; MRE, magnetic resonance elastography; MRI-PDFF, MRI-proton density fat fraction; NAS, non-alcoholic fatty liver disease activity score; NASH, non-alcoholic steatohepatitis; PC3X, crosslinked ADAMTS-2-released N-terminal type III collagen propeptide; PGBF, pegbelfermin; PRO-C3, monomeric ADAMTS-2-released N-terminal type III collagen propeptide; TG, triglycerides.

groups of patient responses were identified in the resulting heatmap. In group 1 (Fig. 6), patients were predominately primary endpoint non-responders and did not have consistent biomarker responses across most assessments either; most patients who received placebo were in this group. Conversely, group 4 consisted primarily of patients who were primary endpoint responders and exhibited concordant improvements in other histological measures and imaging and blood-based biomarkers; all but one of these patients received PGBF. Group 3 consisted of patients who received PGBF and were primary endpoint non-responders, but who nevertheless generally had improved blood and liver metabolic parameters (including hepatic fat fraction measured by MRI-PDFF), blood-based biomarkers of liver injury (AST, ALT, and CK-18 M30), and several non-invasive fibrosis readouts (liver stiffness measured by MRE, ELF score, and PRO-C3). Group 2 largely consisted of patients who had a primary endpoint response but were much less concordant with imaging and blood-based biomarker improvements; the majority of patients in this group had received PGBF, although there were some patients from the placebo arm who were also included.

To further assess which biomarkers might best associate with treatment responses, week 24 biomarker changes were analyzed for correlations with week 24 changes in NASH CRN fibrosis stage and total NAS. Correlations were observed between changes in total NAS and changes in some biomarkers, such as hepatic fat fraction measured by MRI-PDFF, adiponectin, PC3X, ELF, and SomaSignal ballooning (Fig. 7). However, correlations were not observed between biomarkers and fibrosis stage changes for most biomarkers analyzed (Figs S3 and S4).

Discussion

In the FALCON 1 study in patients with NASH and stage 3 fibrosis, approximately twice as many patients who received PGBF had ≥1 stage improvement in fibrosis (by NASH CRN fibrosis score) without NASH worsening or NASH improvement (by NAS) with no worsening of fibrosis (by NASH CRN fibrosis score) compared with those who received placebo.[27] FALCON 1 did not meet its primary endpoint that was designed to test for dose-dependent PGBF response rates; however, non-invasive measures demonstrated that PGBF treatment was associated with improvements in steatosis, injury/inflammation, and fibrosis. Given the known limitations associated with liver biopsy and the challenges associated with histological assessment of liver fibrosis, this FALCON 1 *post hoc* analysis was intended to provide a more thorough investigation into the effect of PGBF on NASH-related biomarkers and to assess potential associations between biomarker responses and histologically determined endpoints.

Steatosis, liver injury and inflammation, and fibrosis are key components of NASH and numerous blood-based biomarkers assessed in this study provided evidence of improvements in each component with PGBF compared with placebo. Serum adiponectin concentrations, which have previously been shown to inversely correlate with steatosis, inflammation, and fibrosis, peaked 4 weeks after initiation of PGBF treatment. This short time frame in which maximal PGBF effects were observed on adiponectin relative to other biomarkers indicates target engagement and reflects the antisteatotic effects of PGBF. The observed increases in adiponectin concentration were similar in magnitude to those observed in phase II trials in NAFLD[37] and

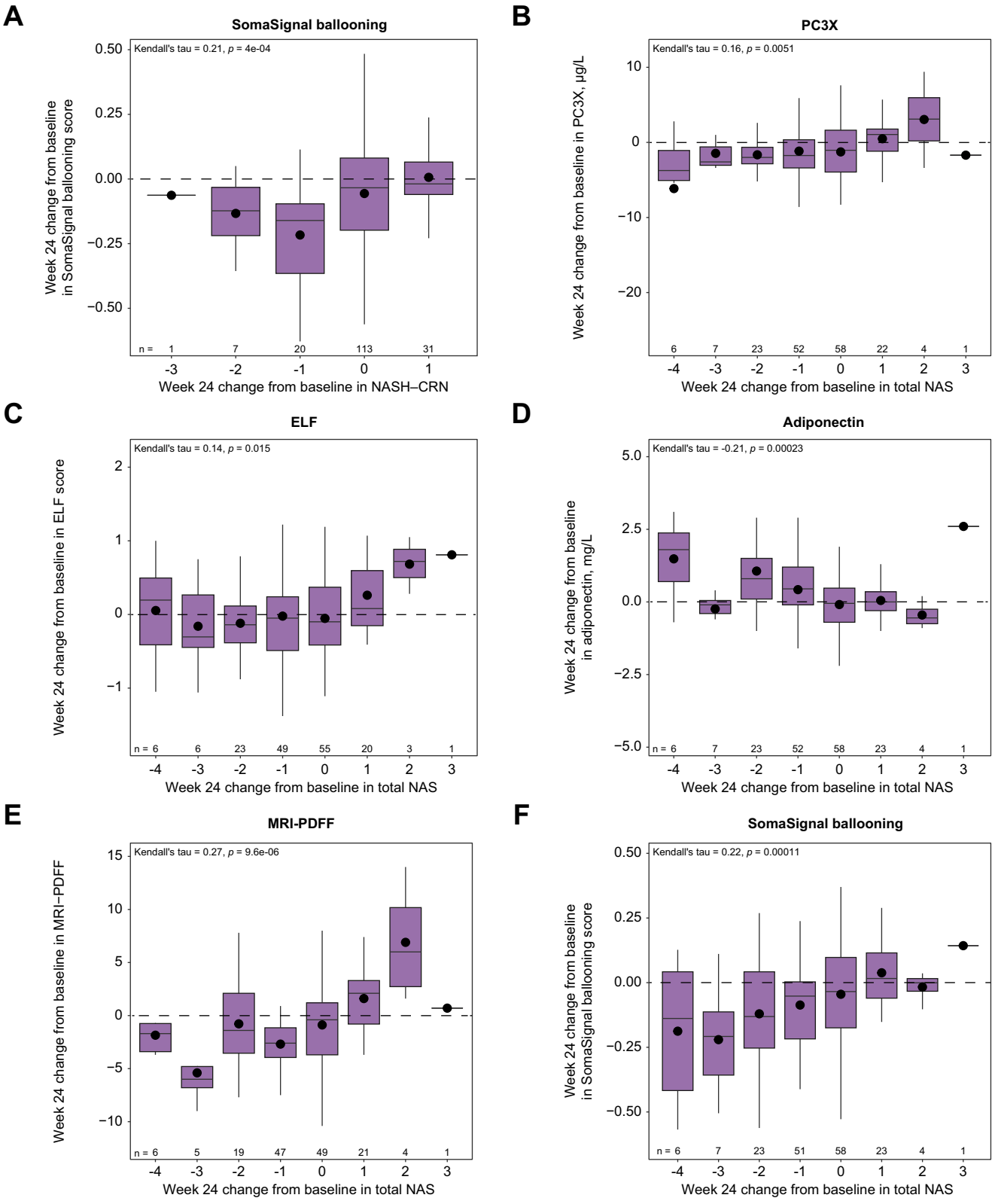

Fig. 7. Correlative analysis between week 24 biomarker changes and week 24 changes in NASH CRN and total NAS. (A) NASH CRN and (B–F) total NAS. Plots show mean (dots), median (bold line), IQR (top and bottom lines of box) and range excluding any outliers over 1.5x IQR (whiskers). Differences in numbers for some NAS stage groups across biomarkers are reflective of differences in data availability. ELF, enhanced liver fibrosis; IQR, interquartile range; MRI-PDFF, MRI-proton density fat fraction; NAS, non-alcoholic fatty liver disease activity score; NASH CRN, non-alcoholic steatohepatitis clinical research network; PC3X, crosslinked ADAMTS-2-released N-terminal type III collagen propeptide.

T2D,[38] and despite the attenuation over the course of the study, mean adiponectin concentrations remained consistently higher across all PGBF arms compared with the placebo arm through week 24. An analogous pattern was observed for CK-18 M30 concentrations, which reflect hepatocyte apoptosis. Here, reductions in CK-18 M30 concentrations were observed in all PGBF arms compared with the placebo arm, beginning at week 8 and maintained through week 24.

Significant PGBF-related improvements were observed at week 24 in the composite fibrosis scores, ELF, FIB-4, and APRI, which have previously been shown to be predictive of disease progression in patients with NAFLD.[35,36] More recently, the ELF test received US Food and Drug Administration approval for assessing the risk of NASH progression to cirrhosis. Biomarkers of fibrogenesis, PRO-C3 and PC3X, were also significantly reduced with PGBF treatment. PRO-C3 has been evaluated in NASH trials as a diagnostic marker of significant fibrosis, as well as a dynamic biomarker of treatment response.[39] Measurement of PC3X to evaluate the pharmacodynamic effects of PGBF was a novel aspect of this study. The PC3X fragment differs from PRO-C3 in that it is thought to be generated on collagen crosslinking, as an alternative measure of matrix stiffness in more advanced stages of liver fibrosis, but it has not yet been well characterized in patients with NASH. PC3X has been shown to predict disease progression in advanced alcoholic steatohepatitis[40] and is also prognostic in hepatocellular carcinoma.[17] The reduction of serum PC3X by PGBF observed in this study is consistent with that observed in a smaller study of patients with NASH treated with an FGF19 analogue.[41]

To build on the individual biomarker data, SomaSignal tests were used to evaluate validated blood-based protein signatures associated with NASH steatosis, inflammation, ballooning, and fibrosis. To our knowledge, this is the first use of SomaSignal to monitor pharmacodynamic effects in a NASH clinical trial. These tests suggested that improvements in all four of these hallmark histological characteristics of NASH were observed in more patients who received PGBF compared with placebo, which is broadly consistent with findings obtained by manual scoring of liver biopsy tissue.[27] Of particular interest were the SomaSignal ballooning and fibrosis scores; these tests showed a highly significant PGBF dose response, as well as the highest correlation with Ishak fibrosis stage, NASH CRN fibrosis score, and MRE assessments of liver stiffness relative to all of the blood-based biomarkers evaluated in this study. The better performance of SomaSignal compared with other measures of fibrosis, such as FIB-4 and APRI, may result from the specific development of SomaSignal in the context of NASH, and to the biological relevance of the individual components, even though these were empirically derived. Given the consistency and clear PGBF dose response observed using SomaSignal probability scores for NASH disease severity, further study on the potential use of these tests in NASH clinical trials is warranted.

Imaging analyses of hepatic fat fraction by MRI-PDFF and liver stiffness by MRE provided further insight into their utility in measuring treatment response over time. Compared with placebo at week 24, PGBF treatment resulted in numerical improvements in liver stiffness while hepatic fat fraction was significantly reduced in the pooled PGBF dose arms. These findings support the idea that PGBF acted as a driver of hepatic fat reduction. At week 24, changes in hepatic fat fraction measured by MRI-PDFF were associated with changes in absolute fat percentage in PGBF arms, but not in the placebo arm. The strength of the associations between these methods of measuring hepatic fat corroborate the value of MRI-PDFF as a non-invasive method to track NASH steatosis over time, as has been shown in previous studies.[18,42] Notably, MRI-PDFF measured larger reductions in hepatic fat than were seen by histologically measured absolute fat percentage, which suggests that MRI-PDFF may provide better sensitivity for detecting treatment-related changes in fat than histological assessment.

An important aim of this study was to investigate potential relationships between non-invasive biomarkers and histologically based evaluations. Clustering analyses demonstrated that histological endpoints and non-invasive biomarkers clustered into several clear categories: steatosis (measured histologically, by MRI-PDFF, and with SomaSignal and other blood-based biomarkers) and metabolism (adiponectin, plasma lipoprotein lipids); tissue injury measured by AST, ALT, CK-18 M30, and SomaSignal ballooning; and fibrosis measured by MRE, ELF score, FIB-4, PRO-C3, PC3X, and SomaSignal fibrosis. The primary endpoint was moderately correlated with other biopsy-based assessments and with SomaSignal ballooning and fibrosis, confirming that these blood-based biomarkers may reflect histological changes in disease activity. On the individual patient level, some who received PGBF demonstrated concordant effects between liver biopsy-based and non-invasive assessments of NASH. In other cases, discordance was observed between histologically measured responses and other non-invasive tests and biomarkers. Notably, improvements measured by non-invasive tests and biomarkers were observed in many patients who did not have a primary endpoint response, which raises the possibility that treatment response to PGBF may not have been fully captured by the histologically measured FALCON 1 primary endpoint.

This idea is supported by results of an analysis of correlations between week 24 changes in biomarkers and week 24 changes in either NASH CRN fibrosis stage or total NAS, which is comprised of scores for steatosis, lobular inflammation, and ballooning. Here, changes in NASH CRN fibrosis stage were not significantly correlated with changes in any biomarkers except for SomaSignal ballooning score. These findings differ from those from a similar analysis performed on data from the phase III REGENERATE study[43] in which associations were found between changes in biomarkers and changes in histologically measured fibrosis. In addition to possibly reflecting different drug effects, the differing results reported here for the FALCON 1 trial could also be attributed to the larger sample size of REGENERATE (931 patients *vs.* 197 patients) and the longer treatment period (18 months *vs.* 6 months). In contrast to changes in fibrosis stage, significant correlations were observed between changes in total NAS and changes in biomarkers such as hepatic fat fraction measured by MRI-PDFF, adiponectin, PC3X, ELF, and SomaSignal ballooning. The small sample size of the study and modest treatment effect size prevent firm conclusions being drawn from this analysis; however, these observations align with the clustering and concordance analyses in which the clearest and most concordant effects of PGBF appeared to be in measures of metabolism and liver steatosis, consistent with the primary mechanism of action of PGBF. These results increase confidence that non-invasive tests reflect key mechanistic features of NASH and that the data obtained from such assessments can effectively supplement histological evaluation.

Due to the complex disease pathology of NASH, achieving optimal therapeutic efficacy may require combination

approaches involving drugs targeting more than one biological pathway. In addition to the modest treatment effect of PGBF monotherapy as measured histologically in this advanced NASH patient population, the biomarker data provide a more detailed view on the mechanism of action of PGBF and further support the conclusion that PGBF improves drivers of NASH pathogenesis and fibrosis at week 24. Given that the earliest, most widespread, and most concordant effects of PGBF appear to be on steatosis biomarkers, combining PGBF with a drug targeting a different biological pathway may potentially lead to an increase in the number of patients with advanced NASH who respond to treatment. Of note, though statistically significant antifibrotic effects were observed in biomarkers of fibrosis, the effect sizes are modest in terms of what is expected to be clinically meaningful.

The major limitations of this exploratory *post hoc* analysis include that the analyses presented here were not explicitly prespecified in the protocol, and that the study was not powered to detect significant findings for these analyses. For the correlative and time course analyses, the likelihood of false-negative conclusions was mitigated by application of the Benjamini-Hochberg procedure to control the false discovery rate. Overall, these results should be interpreted only in the context of a population of patients with NASH and histologically assessed stage 3 fibrosis; extrapolation to other patients with NASH or NAFLD should be made with caution. Finally, dynamic changes in NASH biomarkers and the strength of their correlations with histological analyses likely depend on a given treatment's mechanism of action and effect size; thus, further investigation would be required to make conclusions about whether the findings from this PGBF study are generalizable to other drugs.

In summary, this *post hoc* analysis of the FALCON 1 trial demonstrated that PGBF treatment significantly improved multiple, distinct disease-related biomarkers at week 24 in patients with NASH and stage 3 fibrosis. PGBF exerted positive effects on NASH disease activity and fibrosis, predominately through rapid improvement of steatosis and metabolism. In addition, concordant as well as discordant effects of PGBF were observed on liver biopsy-based and non-invasive assessments of NASH. Overall, these data highlight the importance of considering results from non-invasive measures in combination with histologically derived evaluations to gain the most comprehensive insight into dynamic changes in disease activity that may occur as a result of pharmacological treatment of NASH.

Abbreviations

ALT, alanine aminotransferase; APRI, AST-to-platelet ratio index; AST, aspartate aminotransferase; CK-18 M30, caspase-cleaved cytokeratin 18; ELF, enhanced liver fibrosis; FGF21, fibroblast growth factor 21; FIB-4, fibrosis-4 index; MRE, magnetic resonance elastography; MRI-PDFF, MRI-proton density fat fraction; NAFLD, non-alcoholic fatty liver disease; NAS, NAFLD activity score; NASH, non-alcoholic steatohepatitis; P3NP, procollagen-3 N-terminal propeptide; PC3X, crosslinked ADAMTS-2-released N-terminal type III collagen propeptide; PGBF, pegbelfermin; PRO-C3, monomeric ADAMTS-2-released N-terminal type III collagen propeptide; T2D, type 2 diabetes; TG, triglycerides; TIMP-1, tissue inhibitor of metalloproteinases type 1.

Financial support

This study was fully funded by Bristol Myers Squibb.

Conflicts of interest

EA Brown and G Cizza were employees of Bristol Myers Squibb at the time of the study; S Du, J Schwarz, and ED Charles are employees of Bristol Myers Squibb and may own company stock. A Minnich is a consultant for Bristol Myers Squibb. AJ Sanyal has been a consultant for 89Bio, Albireo, Alnylam, Amgen, AstraZeneca, Bristol Myers Squibb, Boehringer Ingelheim, Covance, Eli Lilly, Fractyl Health, Genentech, Genfit, Gilead Sciences, HemoShear, HistoIndex, Intercept Pharmaceuticals, Inventiva Pharma, Janssen Pharmaceuticals, Madrigal Pharmaceuticals, Mallinckrodt, Merck, NGM Biopharmaceuticals, Novartis, Novo Nordisk, PathAI, Pfizer, Poxel, Prosciento, Regeneron, Roche, Salix Pharmaceuticals, Sequana Medical, Siemens, and Terns Pharmaceuticals; received grants from Boehringer Ingelheim, Bristol Myers Squibb, Eli Lilly, Fractyl Health, Gilead Sciences, Inventiva Pharma, Madrigal, Mallinckrodt, Merck, Novartis, and Novo Nordisk; has an ongoing research collaboration with but has received no direct funds from Echosens-Sandhill and Siemens; owns stock in Durect, Exhalenz, Genfit, HemoShear, Indalo Therapeutics, Northsea Therapeutics, Rivus Pharmaceuticals, and Tiziana Life Sciences; and has received royalties from Elsevier and UpToDate. R Loomba has been a consultant for and received grants from Galmed Pharmaceuticals, Madrigal Pharmaceuticals, and NGM Biopharmaceuticals; has been a consultant for Arrowhead Pharmaceuticals, Bird Rock Bio, Celgene, Enanta Pharmaceuticals, Gir Pharmaceuticals, GRI Bio, Metacrine, and Receptos; has received grants from Allergan, Bristol Myers Squibb, Boehringer Ingelheim, Daiichi-Sankyo, Galectin Therapeutics, GE, Genfit, Gilead Sciences, Intercept Pharmaceuticals, Janssen Pharmaceuticals, Merck, Pfizer, Prometheus, Siemens, and Sirius; and is employed by Liponexus. M Karsdal and DJ Leeming own stock in Nordic Bioscience and are among the original inventors and patent holders for assays for PRO-C3. The Mayo Clinic and RL Ehman have intellectual property rights and a financial interest related to MR elastography technology.

Please refer to the accompanying ICMJE disclosure forms for further details.

Authors' contributions

R Loomba, S Du, RL Ehman, M Karsdal, DJ Leeming, and ED Charles: conception or design; AJ Sanyal, R Loomba, and S Du: data acquisition; EA Brown, A Minnich, J Schwarz, RL Ehman, and G Cizza: data analysis. All authors participated in data interpretation and manuscript drafting, review, and editing.

Acknowledgments

Medical writing assistance was provided by Amanda Martin, PhD, and Kendall Foote, PhD, of Medical Expressions (Chicago, IL) and was funded by Bristol Myers Squibb.

Data availability statement

BMS policy on data sharing may be found at https://www.bms.com/researchers-and-partners/independent-research/data-sharing-request-process.html.

Supplementary data

Supplementary data to this article can be found online at https://doi.org/10.1016/j.jhepr.2022.100661.

References

Author names in bold designate shared co-first authorship

[1] Chalasani N, Younossi Z, Lavine JE, Charlton M, Cusi K, Rinella M, et al. The diagnosis and management of nonalcoholic fatty liver disease: practice guidance from the American Association for the Study of Liver Diseases. Hepatology 2018;67:328–357.

[2] Hagstrom H, Nasr P, Ekstedt M, Hammar U, Stal P, Hultcrantz R, et al. Fibrosis stage but not NASH predicts mortality and time to development of severe liver disease in biopsy-proven NAFLD. J Hepatol 2017;67:1265–1273.

[3] Angulo P, Kleiner DE, Dam-Larsen S, Adams LA, Bjornsson ES, Charatcharoenwitthaya P, et al. Liver fibrosis, but no other histologic features, is associated with long-term outcomes of patients with nonalcoholic fatty liver disease. Gastroenterology 2015;149:389–397.

[4] Taylor RS, Taylor RJ, Bayliss S, Hagstrom H, Nasr P, Schattenberg JM, et al. Association between fibrosis stage and outcomes of patients with nonalcoholic fatty liver disease: a systematic review and meta-analysis. Gastroenterology 2020;158:1611–1625. e1612.

[5] Estes C, Razavi H, Loomba R, Younossi Z, Sanyal AJ. Modeling the epidemic of nonalcoholic fatty liver disease demonstrates an exponential increase in burden of disease. Hepatology 2018;67:123–133.

[6] Noureddin M, Sanyal AJ. Pathogenesis of NASH: the impact of multiple pathways. Curr Hepatol Rep 2018;17:350–360.

[7] Dufour JF, Caussy C, Loomba R. Combination therapy for non-alcoholic steatohepatitis: rationale, opportunities and challenges. Gut 2020;69:1877–1884.

[8] Loomba R. Role of noninvasive biomarkers in the diagnosis of nonalcoholic steatohepatitis with stage 2 or 3 fibrosis. Gastroenterol Hepatol (N Y) 2020;16:139–141.

[9] Ratziu V, Charlotte F, Heurtier A, Gombert S, Giral P, Bruckert E, et al. Sampling variability of liver biopsy in nonalcoholic fatty liver disease. Gastroenterology 2005;128:1898–1906.

[10] Davison BA, Harrison SA, Cotter G, Alkhouri N, Sanyal A, Edwards C, et al. Suboptimal reliability of liver biopsy evaluation has implications for randomized clinical trials. J Hepatol 2020;73:1322–1332.

[11] **Alkhouri N**, **Tincopa M**, Loomba R, Harrison SA. What does the future hold for patients with nonalcoholic steatohepatitis: diagnostic strategies and treatment options in 2021 and beyond? Hepatol Commun 2021;5:1810–1823.

[12] Heyens LJM, Busschots D, Koek GH, Robaeys G, Francque S. Liver fibrosis in non-alcoholic fatty liver disease: from liver biopsy to non-invasive biomarkers in diagnosis and treatment. Front Med (Lausanne) 2021;8:615978.

[13] Castera L, Friedrich-Rust M, Loomba R. Noninvasive assessment of liver disease in patients with nonalcoholic fatty liver disease. Gastroenterology 2019;156:1264–1281. e1264.

[14] Erhardtsen E, Guldager D, Rasmussen K, Manon-Jensen T, Frederiksen P, Leeming D, et al. The liver fibrosis marker PRO-C3 increases with fibrosis stage and is neither elevated in diabetics without liver disease nor in healthy obese subjects [abstract]. J Hepatol 2021;75:S573.

[15] Luo Y, Oseini A, Gagnon R, Charles ED, Sidik K, Vincent R, et al. An evaluation of the collagen fragments related to fibrogenesis and fibrolysis in nonalcoholic steatohepatitis. Sci Rep 2018;8:12414.

[16] Bril F, Leeming DJ, Karsdal MA, Kalavalapalli S, Barb D, Lai J, et al. Use of plasma fragments of propeptides of type III, V, and VI procollagen for the detection of liver fibrosis in type 2 diabetes. Diabetes Care 2019;42:1348–1351.

[17] Jensen C, Holm Nielsen S, Eslam M, Genovese F, Nielsen MJ, Vongsuvanh R, et al. Cross-linked multimeric pro-peptides of type III collagen (PC3X) in hepatocellular carcinoma - a biomarker that provides additional prognostic value in AFP positive patients. J Hepatocell Carcinoma 2020;7:301–313.

[18] Loomba R, Neuschwander-Tetri BA, Sanyal A, Chalasani N, Diehl AM, Terrault N, et al. Multicenter validation of association between decline in MRI-PDFF and histologic response in NASH. Hepatology 2020;72:1219–1229.

[19] Patel J, Bettencourt R, Cui J, Salotti J, Hooker J, Bhatt A, et al. Association of noninvasive quantitative decline in liver fat content on MRI with histologic response in nonalcoholic steatohepatitis. Therap Adv Gastroenterol 2016;9:692–701.

[20] Ostroff R, Alexander L, Williams S. A liquid liver biopsy: serum protein patterns of liver steatosis, inflammation, hepatocyte ballooning and fibrosis in NAFLD and NASH [abstract]. Presented at AASLD 2020. Abstract LP11.

[21] Talukdar S, Kharitonenkov A. FGF19 and FGF21: in NASH we trust. Mol Metab 2021;46:101152.

[22] Kharitonenkov A, Shiyanova TL, Koester A, Ford AM, Micanovic R, Galbreath EJ, et al. FGF-21 as a novel metabolic regulator. J Clin Invest 2005;115:1627–1635.

[23] Polyzos SA, Kountouras J, Zavos C, Tsiaousi E. The role of adiponectin in the pathogenesis and treatment of non-alcoholic fatty liver disease. Diabetes Obes Metab 2010;12:365–383.

[24] Holland WL, Adams AC, Brozinick JT, Bui HH, Miyauchi Y, Kusminski CM, et al. An FGF21-adiponectin-ceramide axis controls energy expenditure and insulin action in mice. Cell Metab 2013;17:790–797.

[25] Charles ED, Neuschwander-Tetri BA, Pablo Frias J, Kundu S, Luo Y, Tirucherai GS, et al. Pegbelfermin (BMS-986036), PEGylated FGF21, in patients with obesity and type 2 diabetes: results from a randomized phase 2 study. Obesity 2019;27:41–49.

[26] Sanyal A, Charles ED, Neuschwander-Tetri BA, Loomba R, Harrison SA, Abdelmalek MF, et al. Pegbelfermin (BMS-986036), a PEGylated fibroblast growth factor 21 analogue, in patients with non-alcoholic steatohepatitis: a randomised, double-blind, placebo-controlled, phase 2a trial. Lancet 2018;392:2705–2717.

[27] Loomba R, Sanyal AJ, Nakajima A, Neuschwander-Tetri BA, Goodman ZD, Harrison SA, et al. Efficacy and safety of pegbelfermin in patients with nonalcoholic steatohepatitis and stage 3 fibrosis: results from the phase 2, randomized, double-blind, placebo-controlled FALCON 1 study [abstract]. Presented at AASLD 2021. Abstract L05.

[28] Abdelmalek MF, Charles ED, Sanyal AJ, Harrison SA, Neuschwander-Tetri BA, Goodman Z, et al. The FALCON program: two phase 2b randomized, double-blind, placebo-controlled studies to assess the efficacy and safety of pegbelfermin in the treatment of patients with nonalcoholic steatohepatitis and bridging fibrosis or compensated cirrhosis. Contemp Clin Trials 2021;104:106335.

[29] Nielsen MJ, Nedergaard AF, Sun S, Veidal SS, Larsen L, Zheng Q, et al. The neo-epitope specific PRO-C3 ELISA measures true formation of type III collagen associated with liver and muscle parameters. Am J Trans Res 2013;5:303–315.

[30] Kleiner DE, Brunt EM, Van Natta M, Behling C, Contos MJ, Cummings OW, et al. Design and validation of a histological scoring system for nonalcoholic fatty liver disease. Hepatology 2005;41:1313–1321.

[31] R Foundation for Statistical Computing. R: a language and environment for statistical computing. Accessed March 23, 2022. https://www.R-project.org.

[32] Corey KE, Vuppalanchi R, Wilson LA, Cummings OW, Chalasani N, Nash CRN. NASH resolution is associated with improvements in HDL and triglyceride levels but not improvement in LDL or non-HDL-C levels. Aliment Pharmacol Ther 2015;41:301–309.

[33] He L, Deng L, Zhang Q, Guo J, Zhou J, Song W, et al. Diagnostic value of CK-18, FGF-21, and related biomarker panel in nonalcoholic fatty liver disease: a systematic review and meta-analysis. Biomed Res Int 2017;2017:9729107.

[34] Johnson A, DiPietro LA. Apoptosis and angiogenesis: an evolving mechanism for fibrosis. FASEB J 2013;27:3893–3901.

[35] Siddiqui MS, Yamada G, Vuppalanchi R, Van Natta M, Loomba R, Guy C, et al. Diagnostic accuracy of noninvasive fibrosis models to detect change in fibrosis stage. Clin Gastroenterol Hepatol 2019;17:1877–1885. e1875.

[36] Younossi ZM, Felix S, Jeffers T, Younossi E, Nader F, Pham H, et al. Performance of the enhanced liver fibrosis test to estimate advanced fibrosis among patients with nonalcoholic fatty liver disease. JAMA Netw Open 2021;4:e2123923.

[37] Gawrieh S, Noureddin M, Loo N, Mohseni R, Awasty V, Cusi K, et al. Saroglitazar, a PPAR-α/γ agonist, for treatment of NAFLD: a randomized controlled double-blind phase 2 trial. Hepatology 2021 Oct;74:1809–1824.

[38] Hartman ML, Sanyal AJ, Loomba R, Wilson JM, Nikooienejad A, Bray R, et al. Effects of novel dual GIP and GLP-1 receptor agonist tirzepatide on biomarkers of nonalcoholic steatohepatitis in patients with type 2 diabetes. Diabetes Care 2020 Jun;43:1352–1355.

[39] Karsdal MA, Daniels SJ, Holm Nielsen S, Bager C, Rasmussen DGK, Loomba R, et al. Collagen biology and non-invasive biomarkers of liver fibrosis. Liver Int 2020;40:736–750.

[40] Karsdal MA, Nielsen MJ, Thiele M, Genovese F, Madsen BS, Hansen JF, et al. A serological marker of collagen type III crosslinking correlates strongly with severity of liver disease [abstract]. J Hepatol 2016;64:S733.

[41] Harrison SA, Ling L, Trotter JF, Paredes AH, Yan AZ, Beuers U, et al. Aldafermin (NGM282) reduces the cross-linked pro-peptides of type III collagen PRO-C3X, a novel biomarker, in non-alcoholic steatohepatitis and primary sclerosing cholangitis patients [abstract]. J Hepatol 2020;73:S526.

[42] Stine JG, Munaganuru N, Barnard A, Wang JL, Kaulback K, Argo CK, et al. Change in MRI-PDFF and histologic response in patients with nonalcoholic steatohepatitis: a systematic review and meta-analysis. Clin Gastroenterol Hepatol 2021;19:2274–2283. e2275.

[43] Rinella ME, Dufour J-F, Anstee QM, Goodman Z, Younossi Z, Harrison SA, et al. Non-invasive evaluation of response to obeticholic acid in patients with NASH: results from the Regenerate study. J Hepatol 2021;76:536–548.

Journal of Hepatology, Volume ■

Supplemental information

Effect of pegbelfermin on NASH and fibrosis-related biomarkers and correlation with histological response in the FALCON 1 trial

Elizabeth A. Brown, Anne Minnich, Arun J. Sanyal, Rohit Loomba, Shuyan Du, John Schwarz, Richard L. Ehman, Morten Karsdal, Diana J. Leeming, Giovanni Cizza, and Edgar D. Charles

Effect of pegbelfermin on NASH and fibrosis-related biomarkers and correlation with histological response in the FALCON 1 trial

Elizabeth A. Brown, Anne Minnich, Arun J. Sanyal, Rohit Loomba, Shuyan Du, John Schwarz, Richard L. Ehman, Morten Karsdal, Diana J. Leeming, Giovanni Cizza, Edgar D. Charles

Table of contents

Fig. S1. Mean absolute change from baseline to week 24 in HDL and LDL

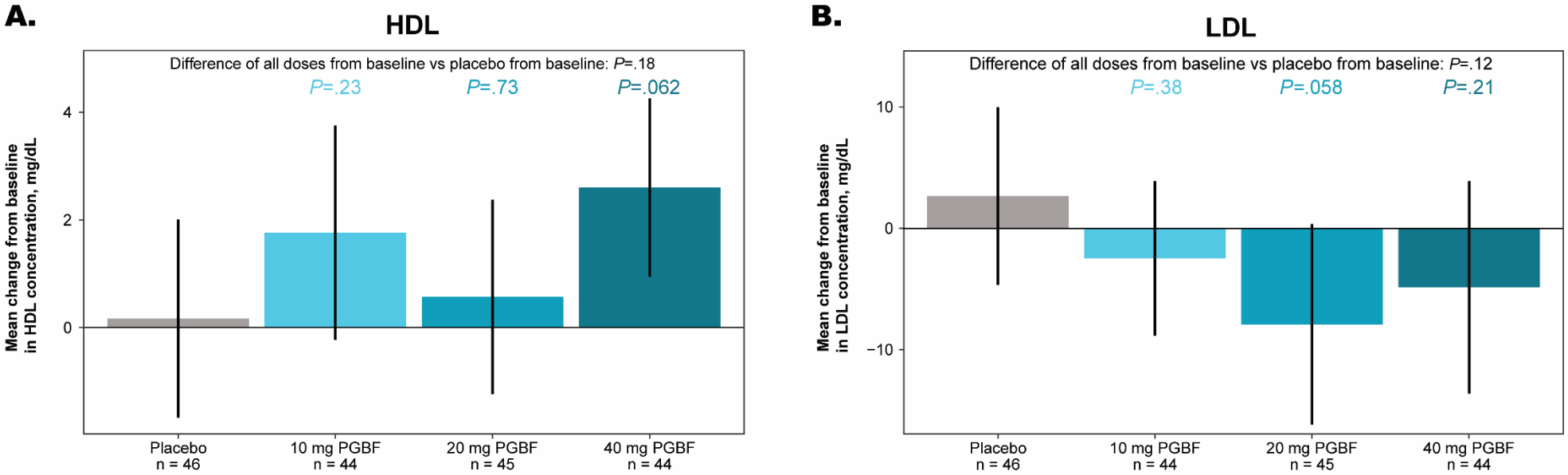

Mean change from baseline ± 95% CI at week 24 is shown. Linear mixed models were fit for each biomarker over time; the difference of each treated arm, and all treated pooled, from baseline compared to placebo from baseline were calculated with *P* values corrected for multiple testing across all tests and biomarkers using the Benjamini-Hochberg procedure.
HDL, high-density lipoprotein; LDL, low-density lipoprotein; PGBF, pegbelfermin.

Fig. S2. Mean absolute change from baseline in ELF score components

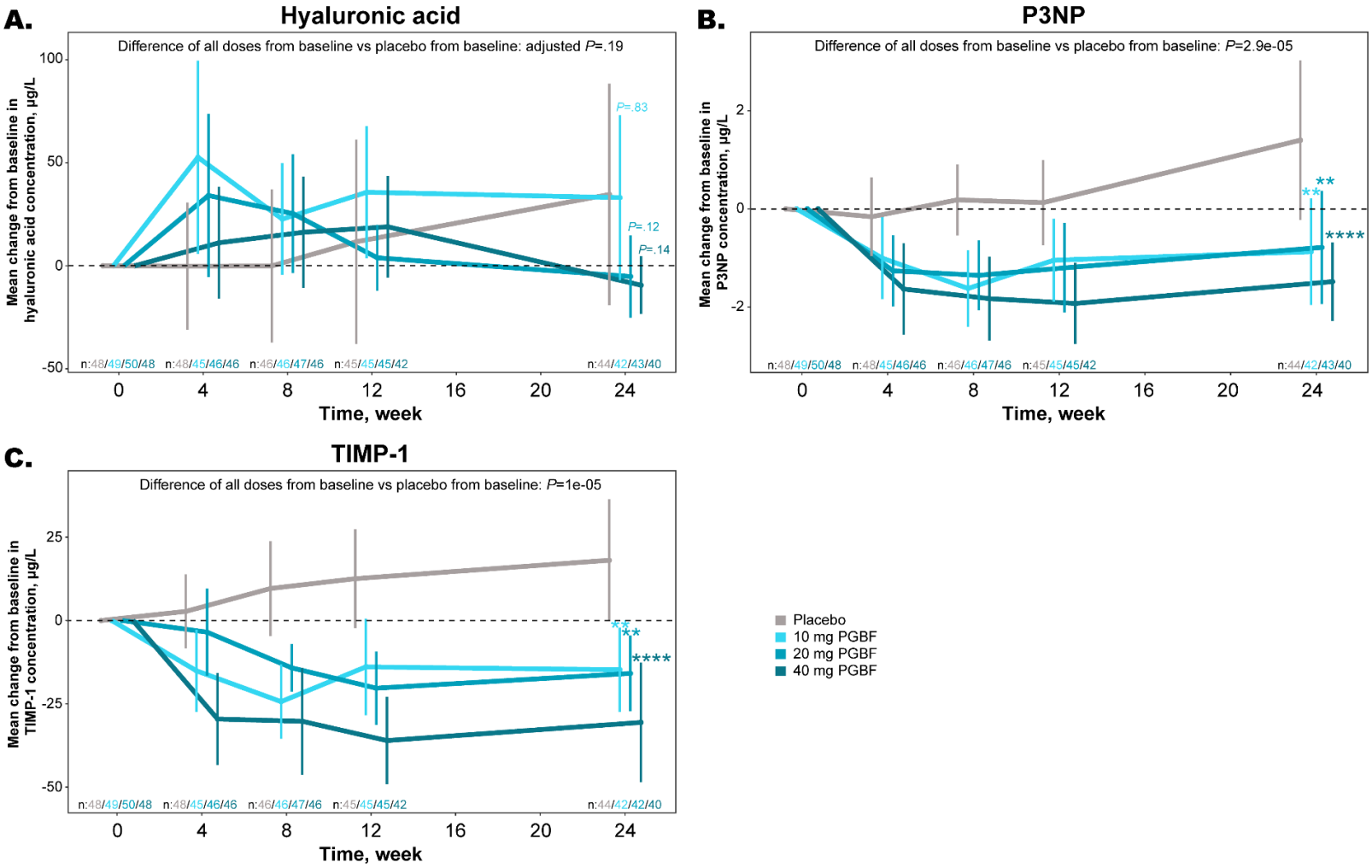

Mean change from baseline at each measured timepoint ± 95% CI is shown. Linear mixed models were fit for each biomarker over time; the difference of each treated arm, and all treated pooled, from baseline compared to placebo from baseline were calculated with *P* values corrected for multiple testing across all tests and biomarkers using the Benjamini-Hochberg procedure. **P*≤ .05; ***P*≤.01, ****P*≤.001, *****P*≤.0001. ELF, enhanced liver fibrosis; P3NP, procollagen-3 N-terminal propeptide; PGBF, pegbelfermin; TIMP-1, tissue inhibitor of metalloproteinases type 1.

Fig. S3. Correlative analysis between week 24 biomarker changes and week 24 NASH CRN fibrosis stage changes

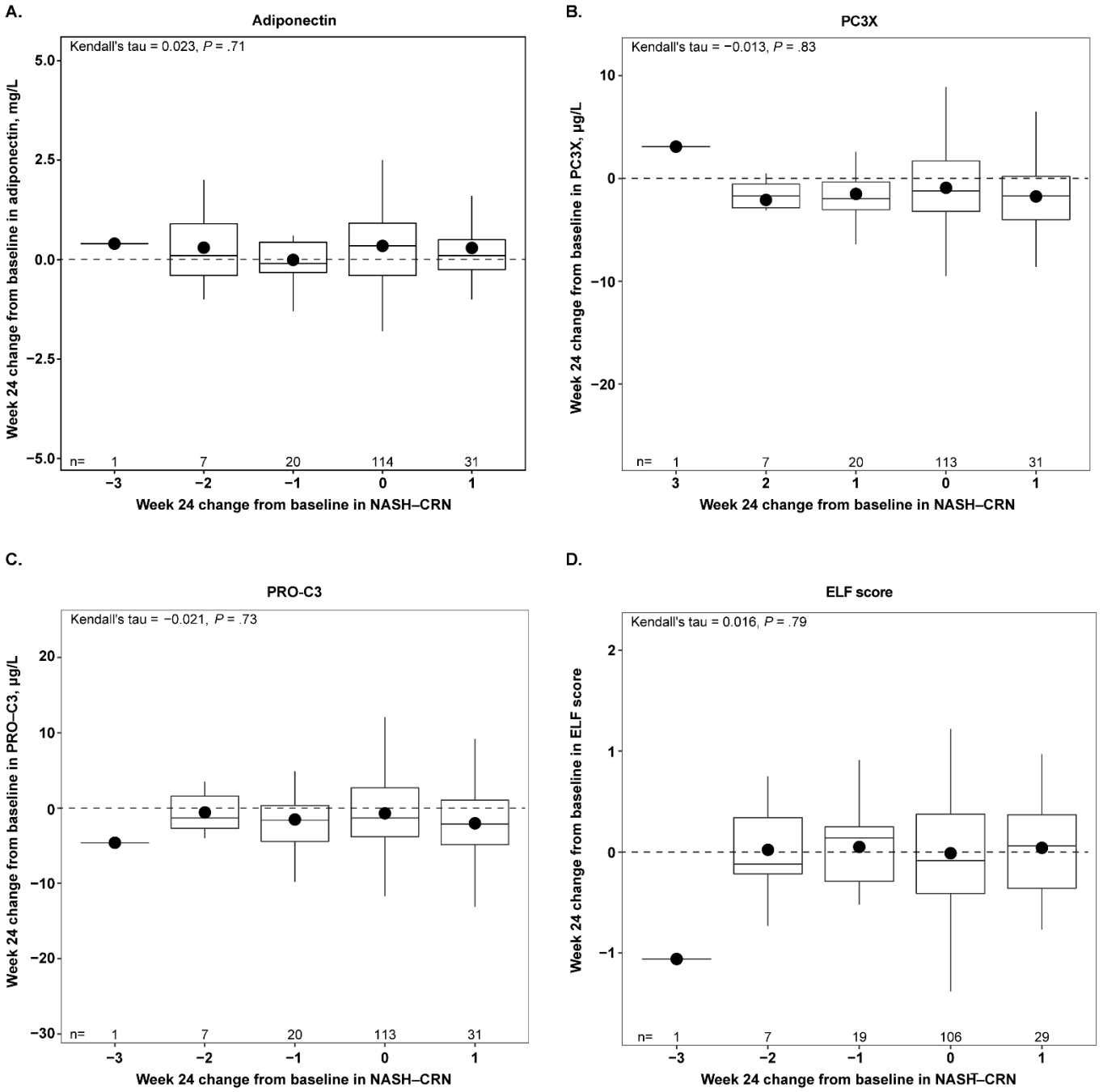

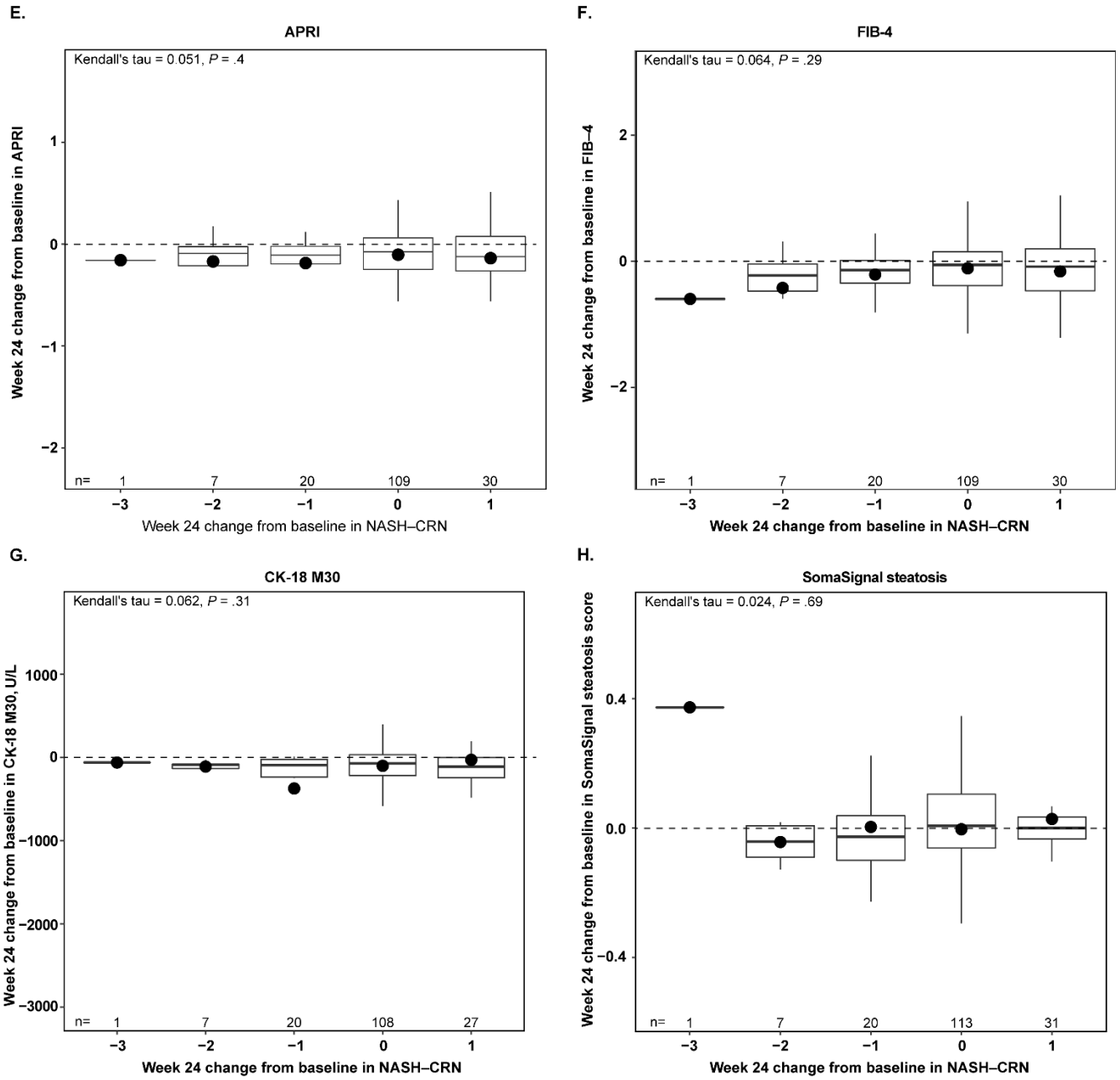
E.
APRI
Kendall's tau = 0.051, P = .4
Week 24 change from baseline in APRI
n= 1 7 20 109 30
Week 24 change from baseline in NASH–CRN
F.
FIB-4
Kendall's tau = 0.064, P = .29
Week 24 change from baseline in FIB–4
n= 1 7 20 109 30
Week 24 change from baseline in NASH–CRN
G.
CK-18 M30
Kendall's tau = 0.062, P = .31
Week 24 change from baseline in CK-18 M30, U/L
n= 1 7 20 108 27
Week 24 change from baseline in NASH–CRN
H.
SomaSignal steatosis
Kendall's tau = 0.024, P = .69
Week 24 change from baseline in SomaSignal steatosis score
n= 1 7 20 113 31
Week 24 change from baseline in NASH–CRN

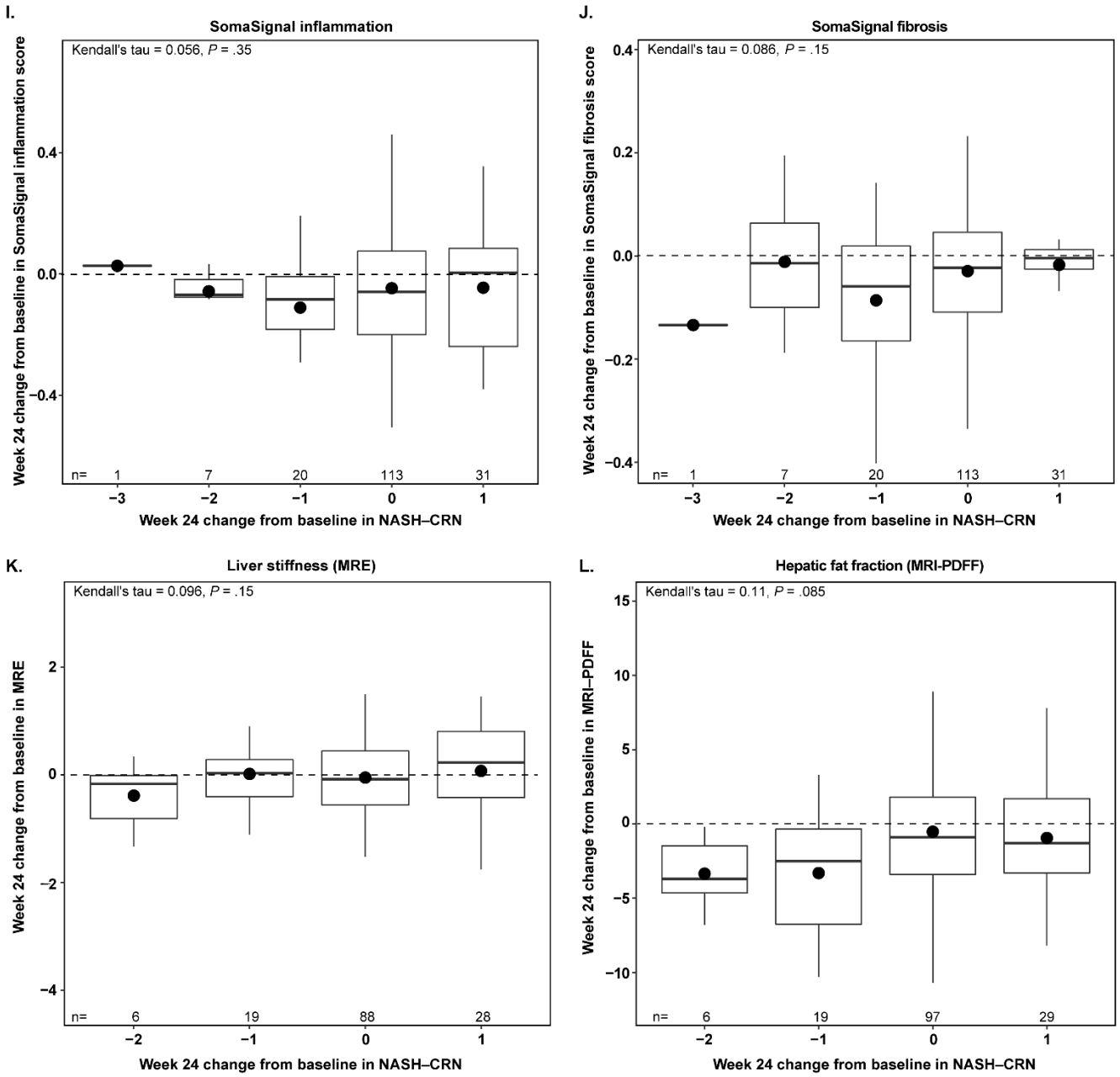

Plots show mean (dots), median (bold line), IQR (top and bottom lines of box) and range excluding any outliers over 1.5x IQR (whiskers). APRI, aspartate aminotransferase-to-platelet ratio index; CK-18 M30, caspase-cleaved cytokeratin 18; ELF, enhanced liver fibrosis; FIB-4, fibrosis-4; MRE, magnetic resonance elastography; MRI-PDFF, magnetic resonance imaging-proton density fat fraction; NASH CRN, nonalcoholic steatohepatitis clinical research network; PC3X, crosslinked ADAMTS-2-released N-terminal type III collagen propeptide; PRO-C3, monomeric ADAMTS-2-released N-terminal type III collagen propeptide.

Fig. S4. Correlative analysis between week 24 biomarker changes and week 24 total NAS changes

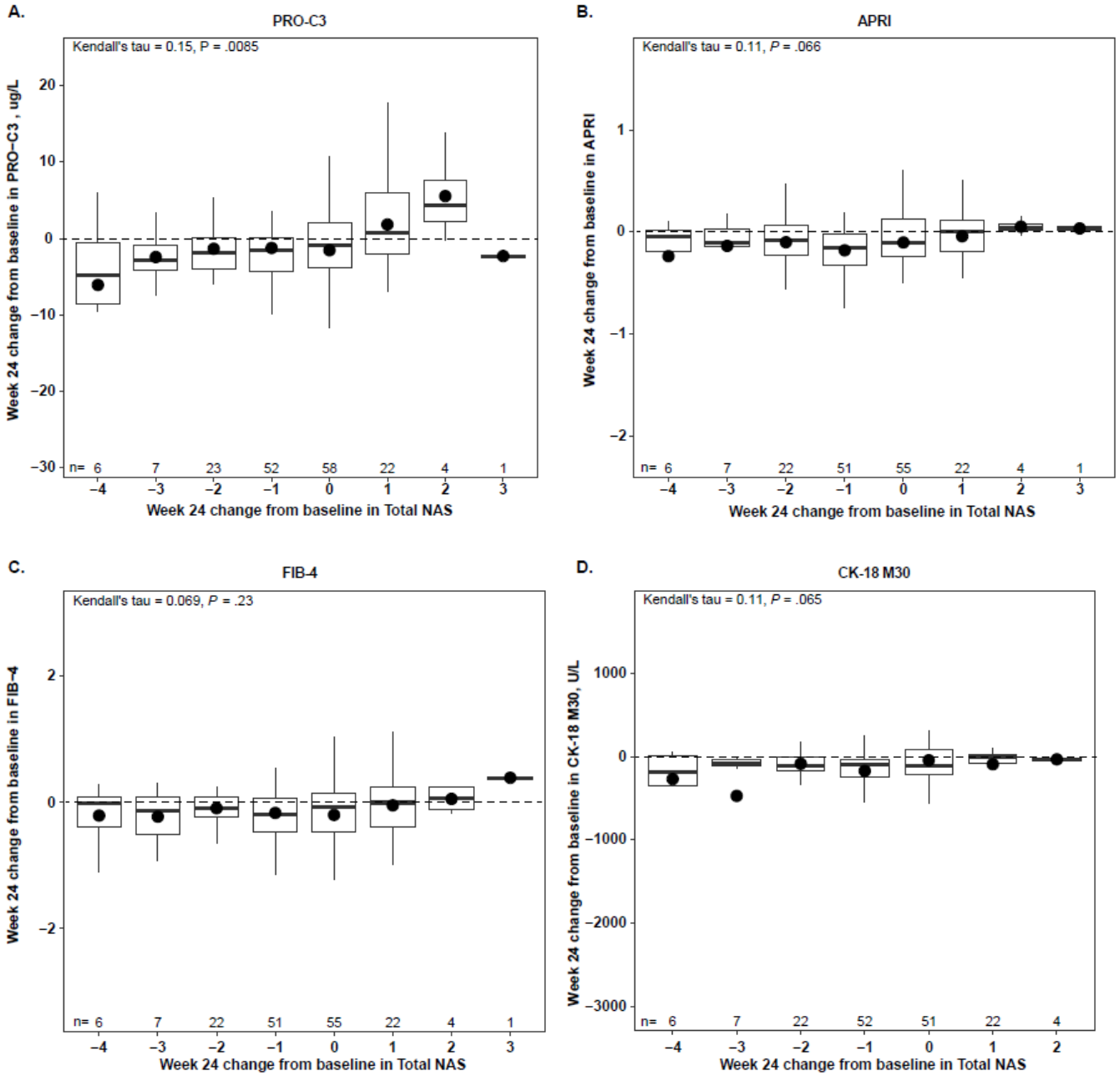

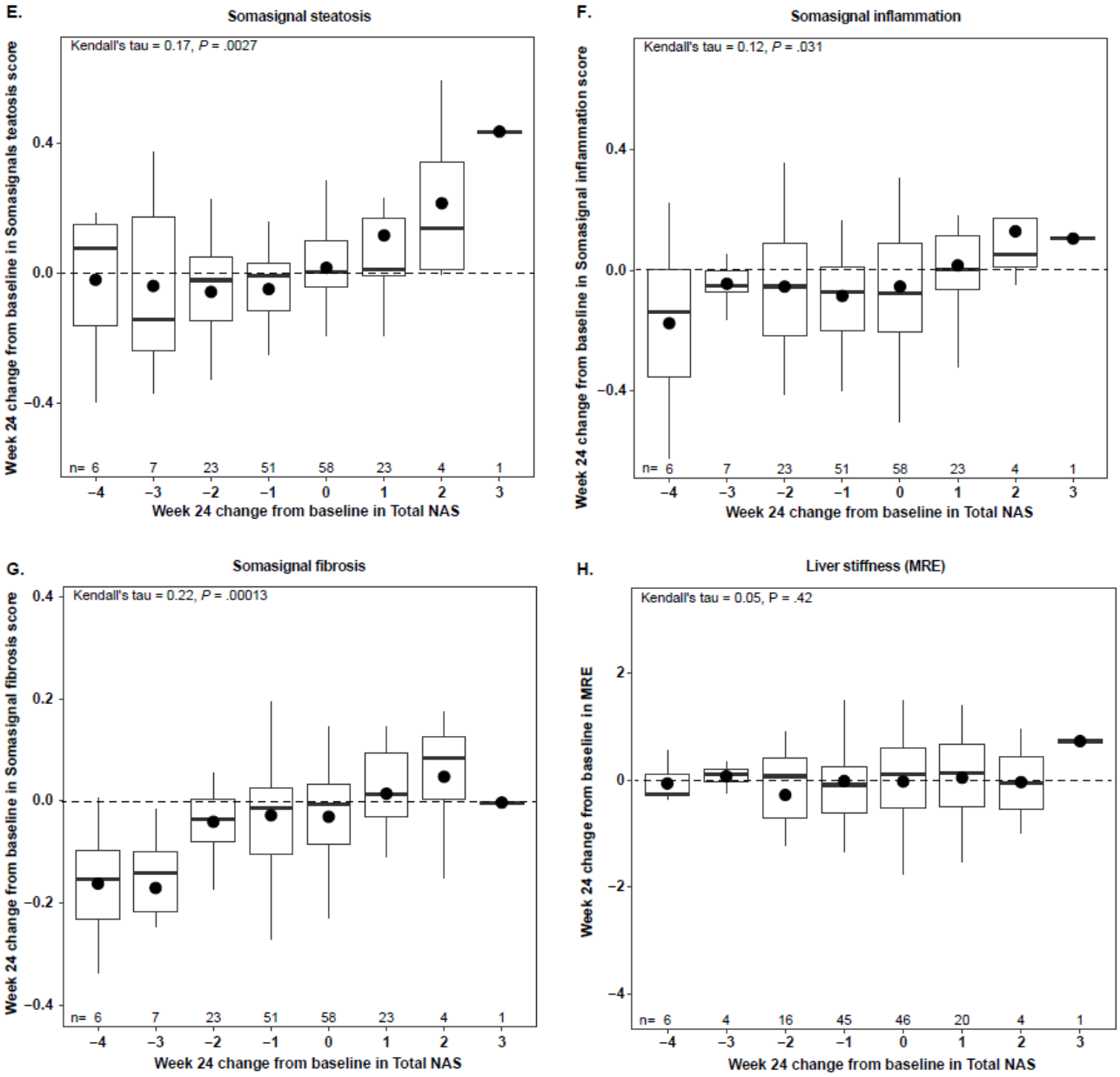

Plots show mean (dots), median (bold line), IQR (top and bottom lines of box) and range excluding any outliers over 1.5x IQR (whiskers). APRI, aspartate aminotransferase-to-platelet ratio index; CK-18 M30, caspase-cleaved cytokeratin 18; FIB-4, fibrosis-4; IQR, interquartile range; MRE, magnetic resonance elastography; NAS, nonalcoholic fatty liver disease activity score; PRO-C3, monomeric ADAMTS-2-released N-terminal type III collagen propeptide.

Table S1. SomaSignal scoring system[1]

Test	Definition[a]	Protein Analytes
NASH ballooning	Predicted probability of NAS steatosis component score of 1, 2, or 3, as opposed to 0	1. aldo-keto reductase family 1 member b10 2. prostaglandin reductase 1 3. adamts-like protein 2 cytotoxic t-lymphocyte protein 4 5. calponin-2
NASH lobular inflammation	Predicted probability of NAS lobular inflammation component score of 2 or 3, as opposed to 0 or 1	1. aminoacylase-1 2. dolichyl-diphospho-oligosaccharide protein glycosyltransferase subunit 1 3. uncharacterized protein c1orf198 4. transcriptional repressor ctcf 5. serum amyloid a-2 protein 6. low affinity immunoglobulin gamma fc region receptor iii-b 7. adiponectin 8. thioredoxin reductase 1 9. maleylacetoacetate isomerase 10. tumor-associated calcium signal transducer 2 11. peptide yy 12. c-c motif chemokine 23 13. procollagen c-endopeptidase enhancer 2 14. low molecular weight phosphotyrosine protein phosphatase
NASH steatosis	Predicted probability of NAS steatosis component score of 1, 2, or 3, as opposed to 0	1. insulin-like peptide insl5 2. fatty acid-binding protein 12 3. atp-dependent dna helicase q1 4. beta-glucuronidase 5. beta-hexosaminidase subunit beta 6. beta-ala-his dipeptidase 7. growth hormone variant 8. prostaglandin reductase 1 9. bpi fold-containing family b member 1

		10. glutamate receptor ionotropic; delta-2 11. serine/threonine-protein kinase/ endoribonuclease ire1
NASH fibrosis	Predicted probability of NASH CRN fibrosis stage 2, 3, or 4, as opposed to 0 or 1	1. adamts-like protein 2 2. complement component c7 3. neurofascin 4. collectin-11 5. vascular endothelial growth factor receptor 6. protein wnt-5 7. procollagen-lysine; 2-oxoglutarate 5-dioxygenase 3 8. fc receptor-like protein 3

[a]For all tests, a probability score of ≥50% is predictive of the specified scoring or staging.
NAS, nonalcoholic fatty liver disease activity score; NASH, nonalcoholic steatohepatitis.

Supplementary reference

1. Ostroff R, Alexander L, Williams S. A liquid liver biopsy: Serum protein patterns of liver steatosis, inflammation, hepatocyte ballooning and fibrosis in NAFLD and NASH [abstract]. Presented at AASLD 2020. Abstract LP11.